framatome

Response to Request for Additional Information - ANP-10337 Supplement 1

Topical Report

November 2019

Copyright © 2019

Framatome Inc.
All Rights Reserved

Nature of Changes

Item	Section(s) or Page(s)	Description and Justification
1	All	Initial Issue

Contents

Framatome Inc.

ANP-10337 Supplement 1Q2NP
Revision 0

Response to Request for Additional Information - ANP-10337 Supplement 1
Topical Report
Page iii

List of Tables

Framatome Inc.

ANP-10337 Supplement 1Q2NP
Revision 0

Response to Request for Additional Information - ANP-10337 Supplement 1
Topical Report
Page iv

List of Figures

Framatome Inc.

ANP-10337 Supplement 1Q2NP
Revision 0

Response to Request for Additional Information - ANP-10337 Supplement 1
Topical Report

Page v

Nomenclature

Acronym	Definition
ASME	American Society of Mechanical Engineers
BOL	Beginning of Life
DGE	Deformable Grid Element
EOL	End of Life
IGM	Intermediate GAIA Mixer
LOCA	Loss of Coolant Accident
NRC	Nuclear Regulatory Commission
RAI	Request for Additional Information
SSE	Safe Shutdown Earthquake

Framatome Inc.

ANP-10337 Supplement 1Q2NP
Revision 0

Response to Request for Additional Information - ANP-10337 Supplement 1
Topical Report

Page vii

INTRODUCTION

The United States Nuclear Regulatory Commission (NRC) provided a request for additional information (RAI) regarding the topical report ANP-10337PA, Supplement 1P-0 (Reference 1) in Reference 2. A total of 11 questions were received from the NRC.

The following sections provide the responses to NRC questions 4, 5, 6, 7, 9, and 10. The responses for the remaining questions were provided in a previously submitted report.

1.0   RAI 4

Question:

Section A.1 describes how directional dependencies are treated in the analysis of test data for candidate spacer grid designs. In particular, the discussion indicates that whenever the dynamic response characterization of a candidate grid design differs depending on the direction of the impact, the most conservative direction is used to define the DGE model in the analysis methodology. Describe the criteria used to determine which direction is the most conservative and discuss how many tests in each direction are needed to provide adequate evidence for a generic conclusion on a spacer grid design.

Response:

The spacer grid dynamic response can depend on the impact direction because of an asymmetric design of the inner grid strips. The asymmetry arises from the arrangement of the interlocking slot pattern of the inner strips. As a result the stiffness, strength, and large-deformation behavior can be different depending on the impact direction. The Deformable Grid Element (DGE) was developed [

            ] are used to determine the more conservative direction to be fully characterized for the lateral seismic / LOCA analysis.

The first criterion used to determine the more conservative test direction is a comparison of the [   ] The more conservative test direction would produce a [

            ] This criterion corresponds to the gradual and progressive increase in residual deformation over the duration of the accident time history.

The second criterion used to determine the more conservative test direction is the

[   ] This quantity

represents the [

                                                                              ]

For a new spacer grid design or a design that has not been studied for directional

dependence, [

                                                                              ]

2.0   RAI 5

Question:

Provide data equivalent to the benchmarking in Appendix B (in particular, Tables B-1, B-3 through B-5 and Figures B-4 through B-8) for the reverse and random impact test protocols, utilizing the same DGE model that is used to generate the data in Appendix B. Whenever possible, provide this data for both beginning of life (BOL) and end of life (EOL). In addition, provide EOL benchmarking data for the progressive impact test protocol. If a different DGE model is used, or the test data used in benchmarking is not consistent with the benchmarking for the DGE model, explain the differences and why they are acceptable.

Response:

It is not possible to provide a comparison to reverse and random impact data utilizing the same DGE model used in Appendix B, because the reverse and random impact tests were performed with a different spacer grid design. The design differences affected the inner strip detailed design, the outer strip design, and the final welded spacer assembly. However, a single progressive impact test was performed in BOL and EOL conditions as part of the reverse and random test campaign, so the same spacer grid design was tested using all three impact test protocols.

Although only one spacer grid was tested with the progressive test protocol, the same benchmarking procedure was used to develop and validate the DGE model. The consequence of using test data from a single test is that the natural variation, or scatter, in the test data is not present, and the DGE model output must match the test data closely to [   ]

BOL Progressive Test Benchmark

Since only one progressive impact test is available, the target behavior for the benchmark is the same as the experimental data, which is provided in Table 2-1. The benchmarked DGE model parameters are listed in Table 2-2. A comparison between the experimental data and the DGE model output is provided in Figure 2-1 through Figure 2-5.

EOL Progressive Test Benchmark

Since only one progressive impact test is available, the target behavior for the benchmark is the same as the experimental data, which is provided in Table 2-3. The benchmarked DGE model parameters are listed in Table 2-4. A comparison between the experimental data and the DGE model output is provided in Figure 2-6 through Figure 2-10.

Statistical Validation of BOL and EOL Progressive Test Benchmark

The Analysis of Covariance results for the BOL and EOL benchmark are provided in Table 2-5 and Table 2-6, respectively. The coefficient of determination for the BOL and EOL benchmark are provided in Table 2-7. The root mean squared error for the BOL and EOL benchmark are provided in Table 2-8.

BOL Reverse Protocol Test Comparison

The same DGE model that was benchmarked to the progressive impact test data was used to simulate a reverse protocol test. The reverse protocol test is characterized by starting the test with a high kinetic energy impact and then incrementally decreasing the impact kinetic energy. The purpose of the test is to confirm that the maximum residual deformation corresponds to the maximum impact force.

Two BOL reverse impact test were performed, and the experimental data is presented in Table 2-9 and Table 2-10. A comparison between the experimental data and the DGE model output is provided in Figure 2-11 through Figure 2-14.

EOL Reverse Protocol Test Comparison

Two EOL reverse impact test were performed, and the experimental data is presented in Table 2-11 and Table 2-12. A comparison between the experimental data and the DGE model output is provided in Figure 2-15 through Figure 2-22.

BOL Random Protocol Test Comparison

The same DGE model that was benchmarked to the progressive impact test data was used to simulate a random protocol test. This test is intended to simulate a realistic sequence of impacts that could occur during a seismic event. One BOL random impact test was performed, and the experimental data is presented in Table 2-13. A comparison between the experimental data and the DGE model output is provided in Figure 2-23 and Figure 2-24.

EOL Random Protocol Test Comparison

One EOL random impact test was performed, and the experimental data is presented in Table 2-14. A comparison between the experimental data and the DGE model output is provided in Figure 2-25 and Figure 2-26.

Discussion

The DGE model, which was benchmarked to progressive impact test data, was used to successfully predict the residual deformation for the reverse and random protocol tests. Table 2-15 presents the predicted and measured residual deformations for the BOL and EOL cases. The additional validation of the DGE performance provides assurance that the residual deformations predicted in the lateral seismic / LOCA analyses are conservative. Additional conservatism is included through the use of a 95% upper confidence limit on the residual deformation.

The progressive impact test provides a data set that is readily applied to the DGE for benchmarking purposes. It is possible, however, that a particular set of input parameters satisfies the progressive test benchmark but does not provide an accurate or conservative prediction for the reverse or random impact tests. It is for this reason that additional dynamic impact tests will be performed to complete the test data base for a DGE benchmark analysis. The additional tests will include the aspects of the reverse and random protocol tests such as relatively large step changes in residual deformation and sequences of impacts below the maximum impact kinetic energy.

Change pages are provided in Section 9 of this document for Section 4.6.2 of the topical report supplement (Reference 1) to add the requirement that a reverse or random type test be included along with the standard progressive impact test for additional validation of the DGE model input parameters.

Framatome Inc.

ANP-10337 Supplement 1Q2NP
Revision 0

Response to Request for Additional Information - ANP-10337 Supplement 1
Topical Report

Page 2-5

Table 2-1 Experimental Data for BOL Progressive Test
(Spacer 116074)

[

Framatome Inc.

ANP-10337 Supplement 1Q2NP
Revision 0

Response to Request for Additional Information - ANP-10337 Supplement 1
Topical Report

Page 2-6

Table 2-2 DGE Input Parameters, BOL Hot

[

]

Framatome Inc.

ANP-10337 Supplement 1Q2NP
Revision 0

Response to Request for Additional Information - ANP-10337 Supplement 1
Topical Report

Page 2-7

**Table 2-3 Experimental Data for EOL Progressive Test
(Spacer 116080)**
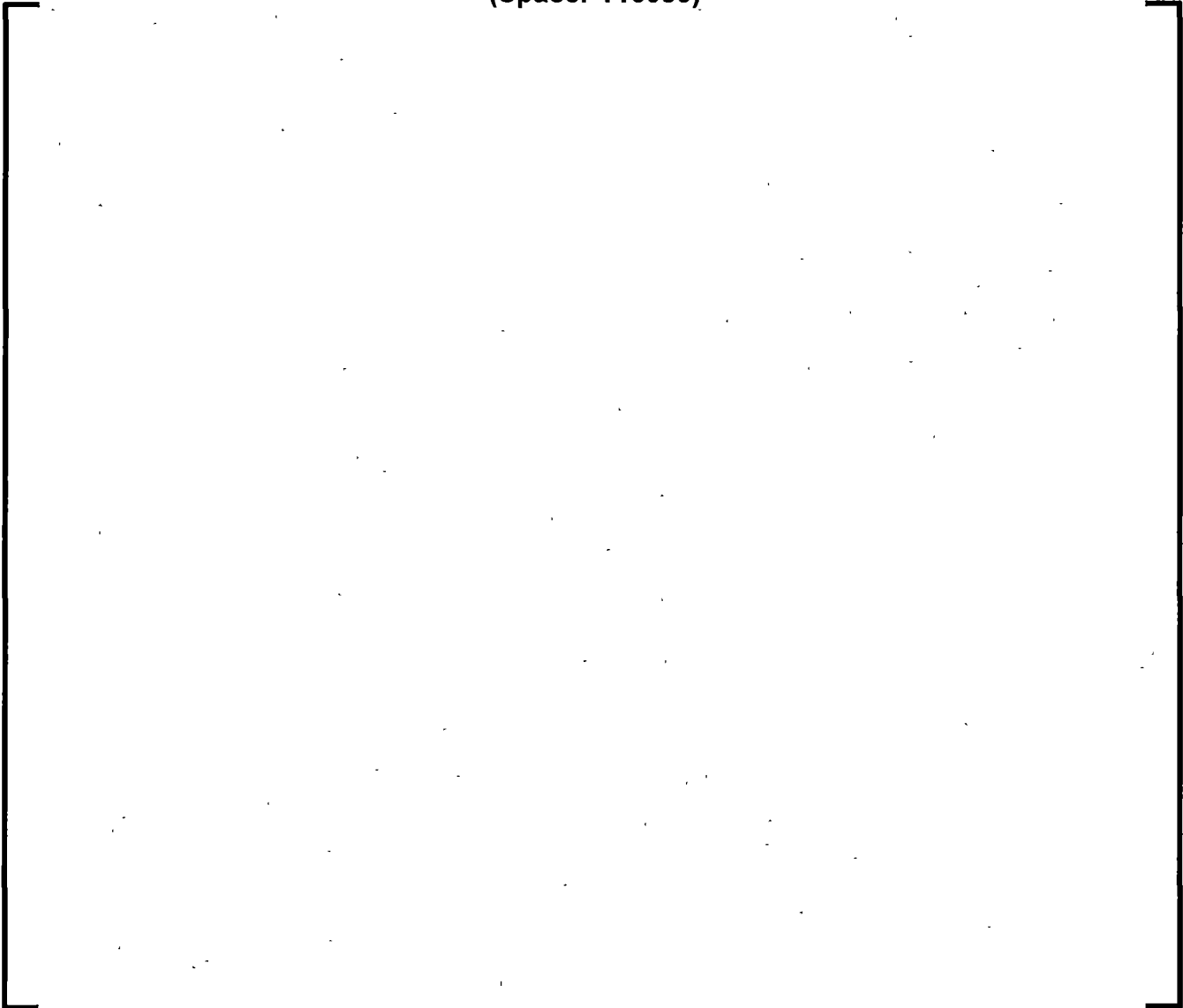
Table 2-4 DGE Input Parameters, EOL Cold

[

]

Framatome Inc.

ANP-10337 Supplement 1Q2NP
Revision 0

Response to Request for Additional Information - ANP-10337 Supplement 1
Topical Report

Page 2-9

Table 2-5 Analysis of Covariance Results, BOL Hot

Table 2-6 Analysis of Covariance Results, EOL Cold

Framatome Inc.

ANP-10337 Supplement 1Q2NP
Revision 0

Response to Request for Additional Information - ANP-10337 Supplement 1
Topical Report

Page 2-10

Table 2-7 Coefficients of Determination

[

]
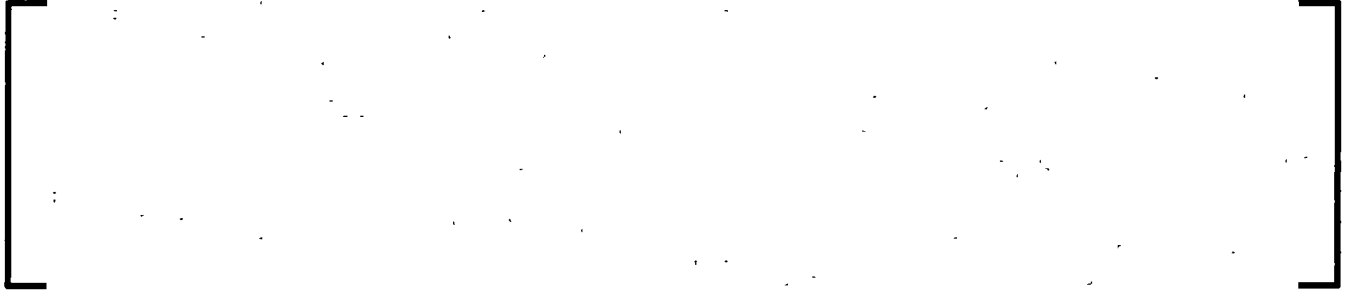
Table 2-8 Root Mean Squared Error

[

]
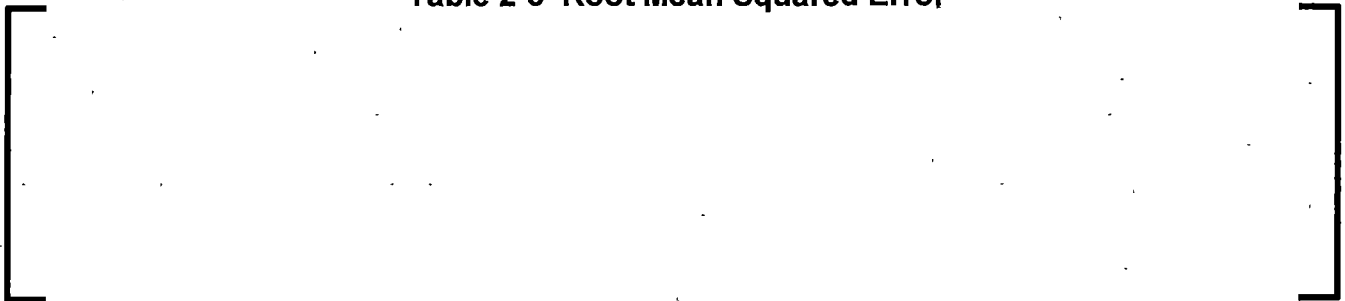
**Table 2-9 Experimental Data for BOL Reverse Protocol Test 1
(Spacer 103677)**
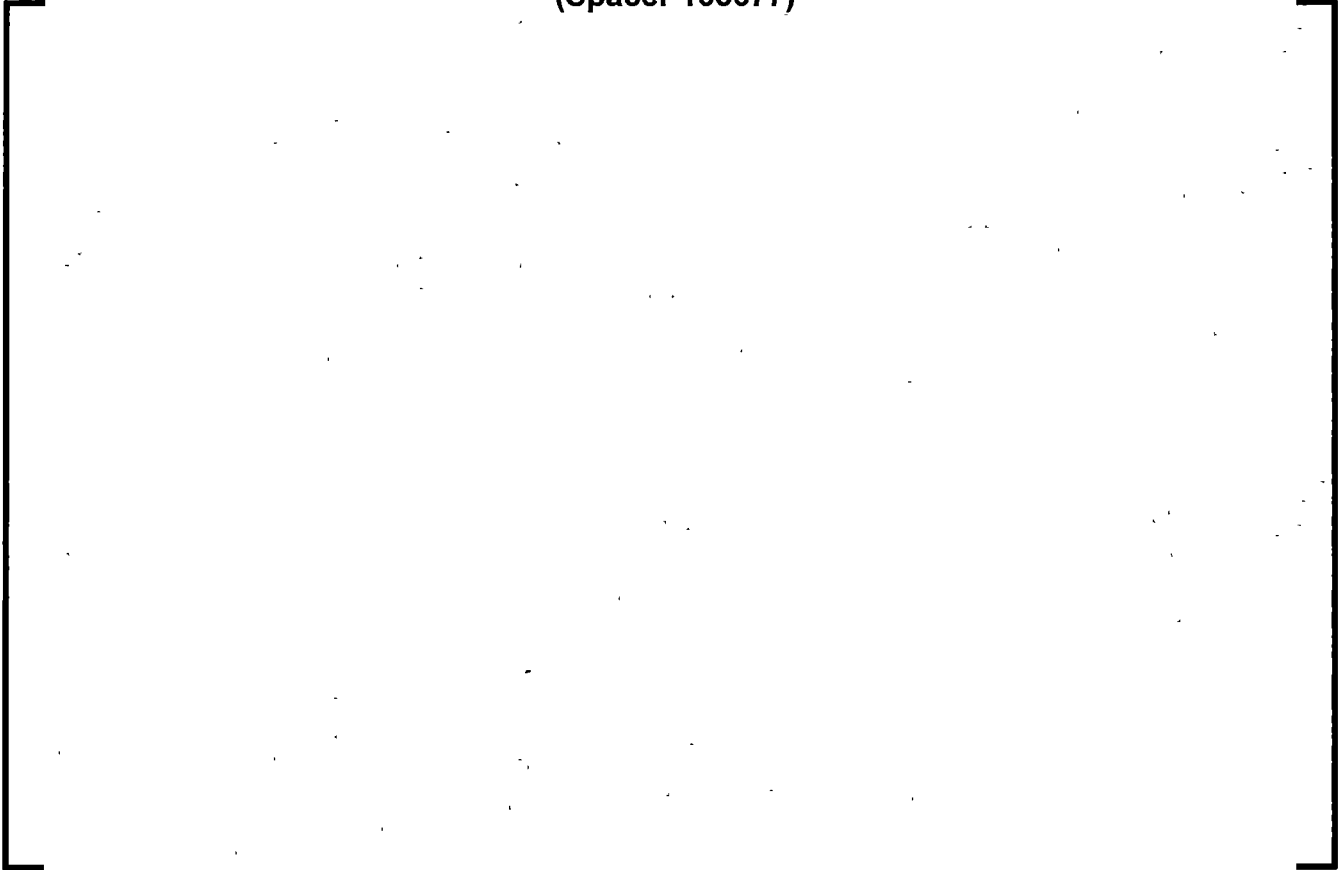
[
]

Framatome Inc.

Response to Request for Additional Information - ANP-10337 Supplement 1
Topical Report

ANP-10337 Supplement 1Q2NP
Revision 0

Page 2-12

**Table 2-10 Experimental Data for BOL Reverse Protocol Test 2
(Spacer 103676)**
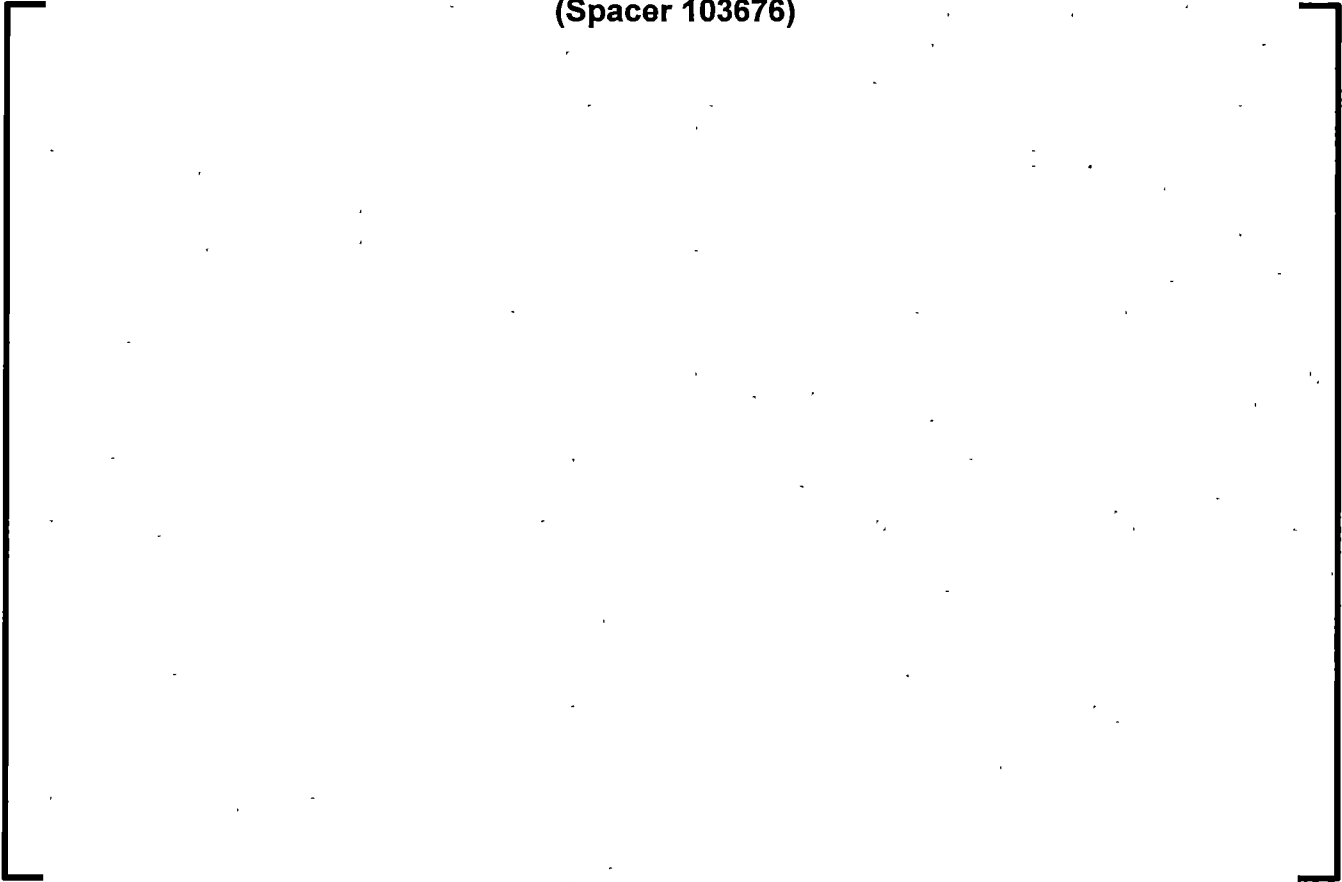
[

]

**Table 2-11 Experimental Data for EOL Reverse Protocol Test 1
(Spacer 103679)**
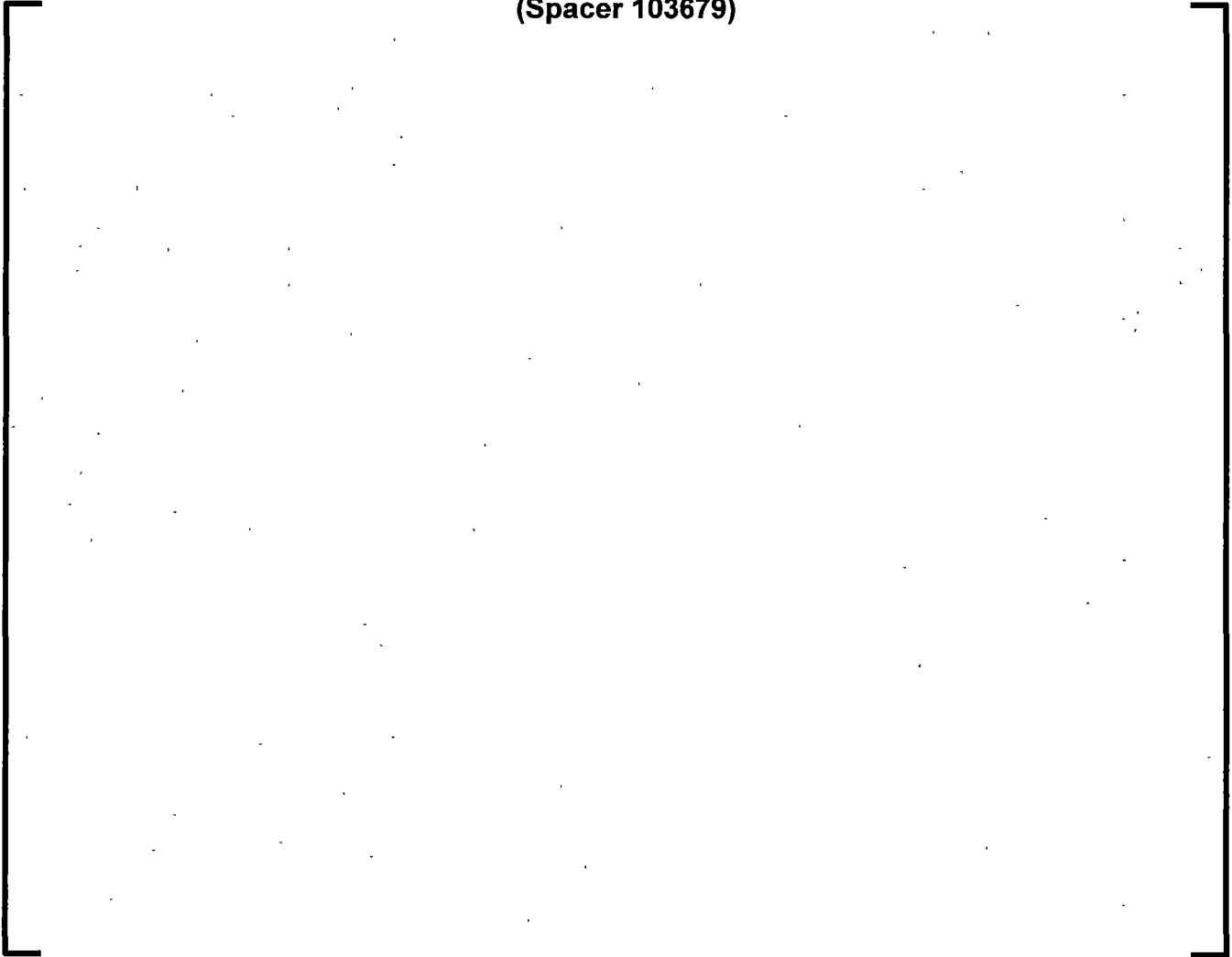
Framatome Inc.

ANP-10337 Supplement 1Q2NP
Revision 0

Response to Request for Additional Information - ANP-10337 Supplement 1
Topical Report

Page 2-14

**Table 2-12 Experimental Data for EOL Reverse Protocol Test 2
(Spacer 103680)**
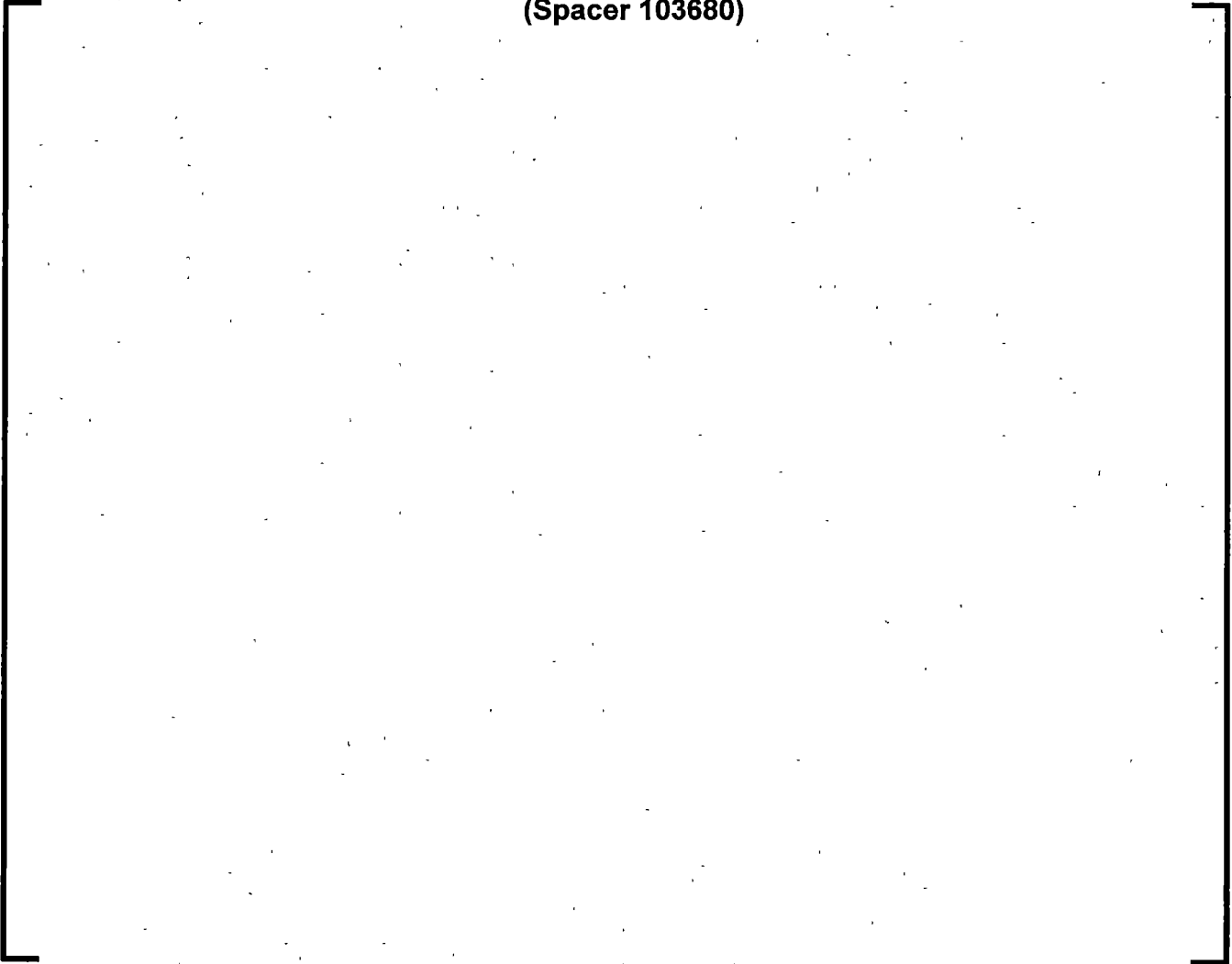
Framatome Inc.

ANP-10337 Supplement 1Q2NP
Revision 0

Response to Request for Additional Information - ANP-10337 Supplement 1
Topical Report

Page 2-15

**Table 2-13 Experimental Data for BOL Random Protocol Test
(Spacer 116077)**

Framatome Inc.

ANP-10337 Supplement 1Q2NP
Revision 0

Response to Request for Additional Information - ANP-10337 Supplement 1
Topical Report

Page 2-16

Framatome Inc.

ANP-10337 Supplement 1Q2NP
Revision 0

Response to Request for Additional Information - ANP-10337 Supplement 1
Topical Report
Page 2-17
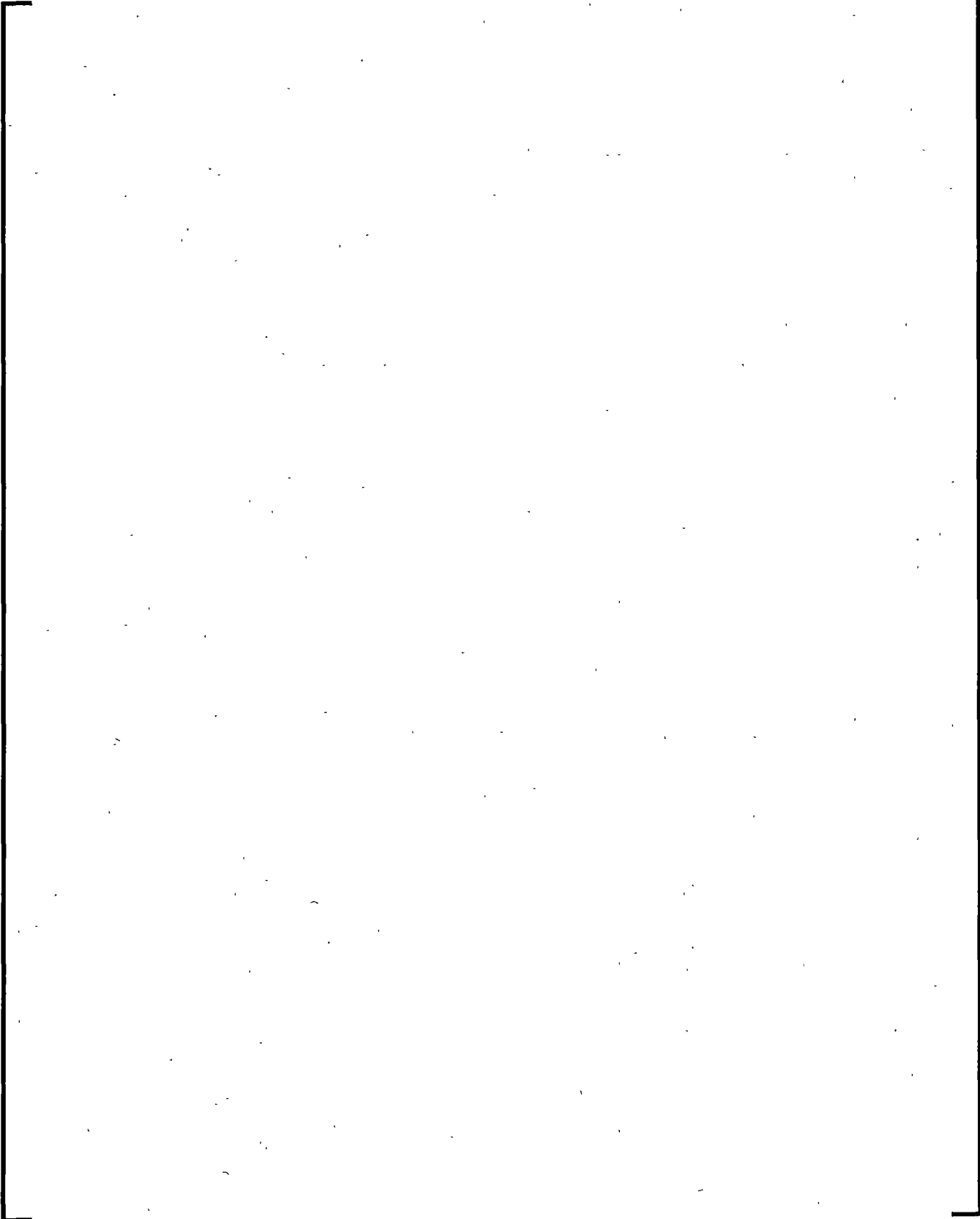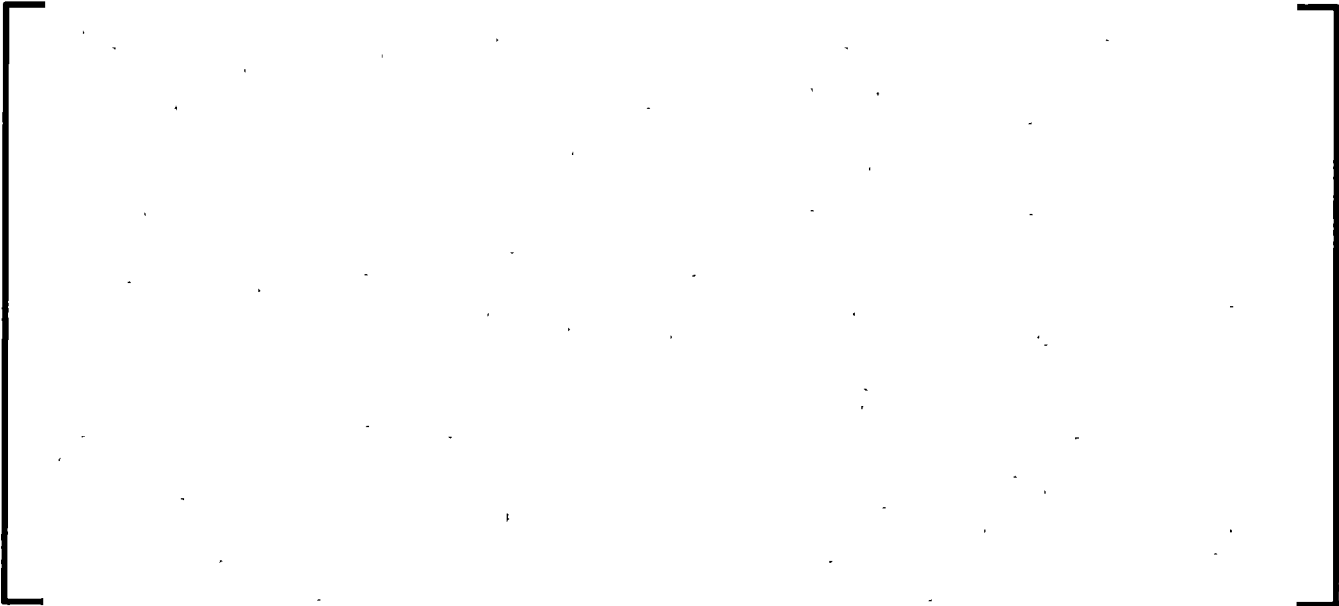
**Table 2-14 Experimental Data for EOL Random Protocol Test
(Spacer 116083)**
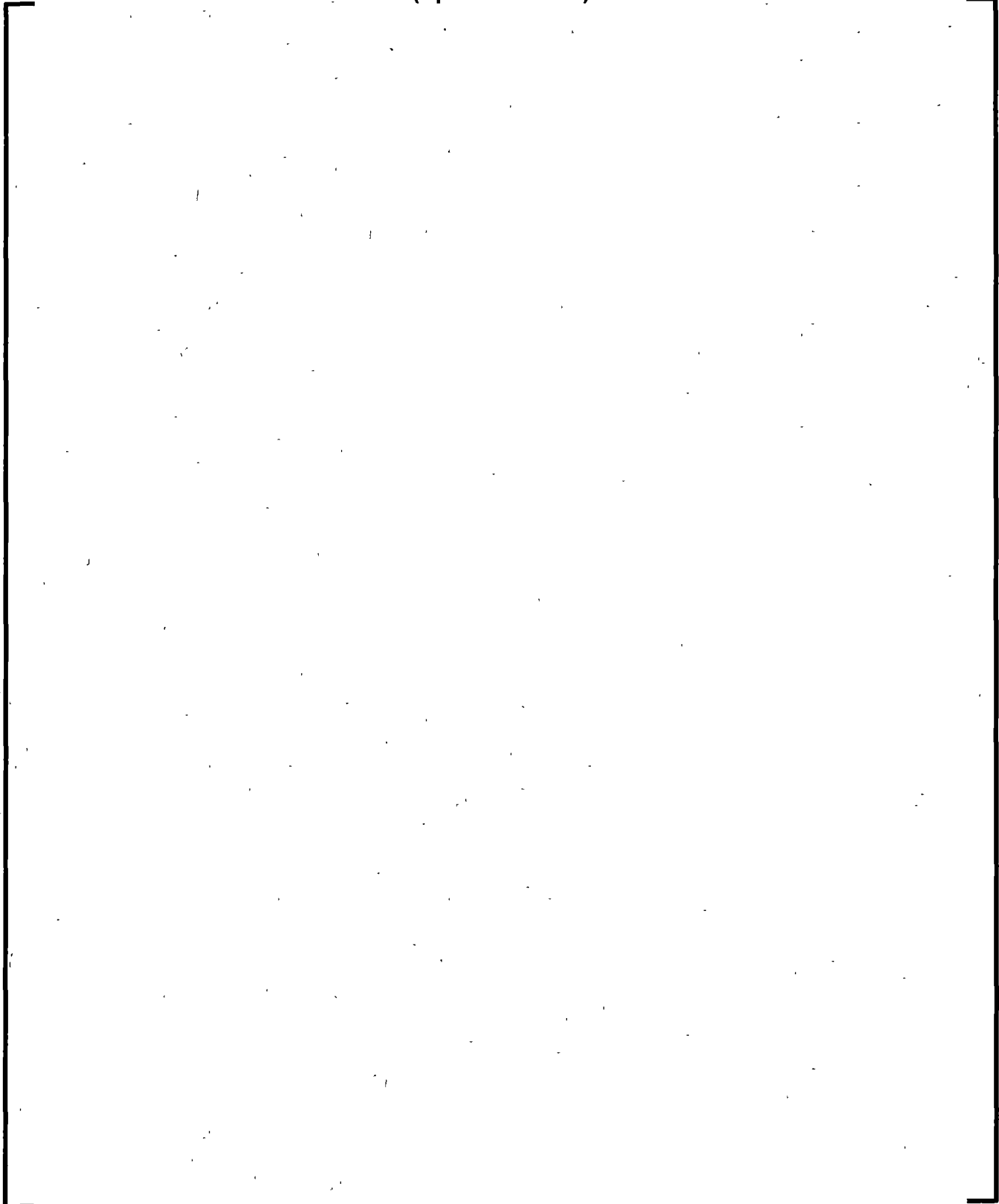
[ ]

Framatome Inc.

ANP-10337 Supplement 1Q2NP
Revision 0

Response to Request for Additional Information - ANP-10337 Supplement 1
Topical Report

Page 2-18

Framatome Inc.

ANP-10337 Supplement 1Q2NP
Revision 0

Response to Request for Additional Information - ANP-10337 Supplement 1
Topical Report

Page 2-19
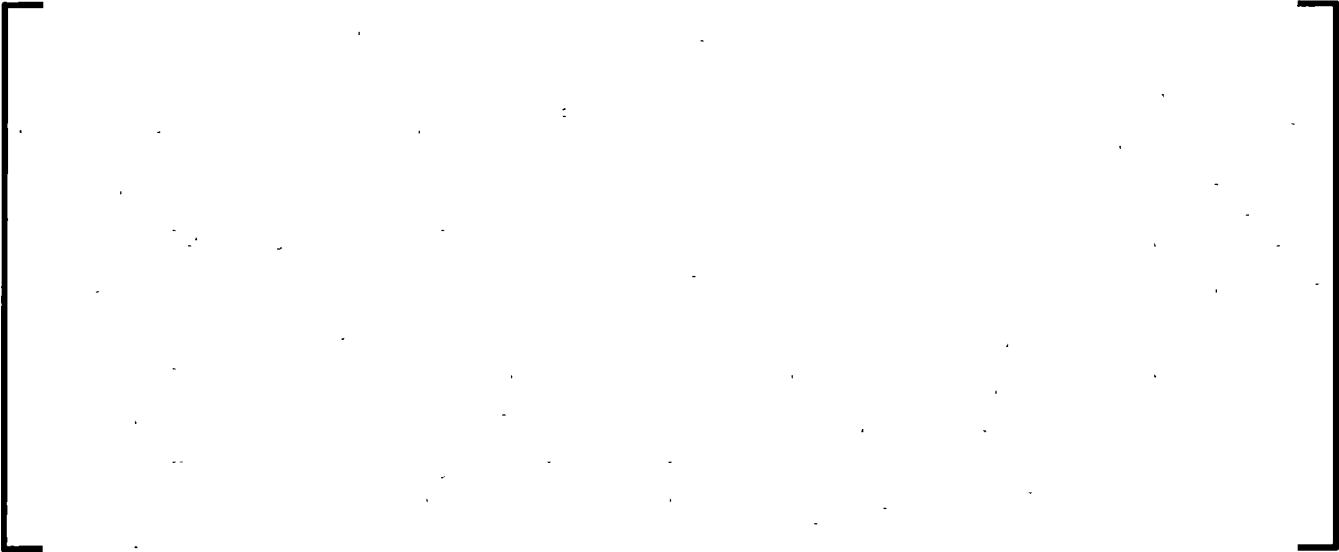
Table 2-15 Measured versus Predicted Residual Deformations

[
]

Framatome Inc.

ANP-10337 Supplement 1Q2NP
Revision 0

Response to Request for Additional Information - ANP-10337 Supplement 1
Topical Report

Page 2-20
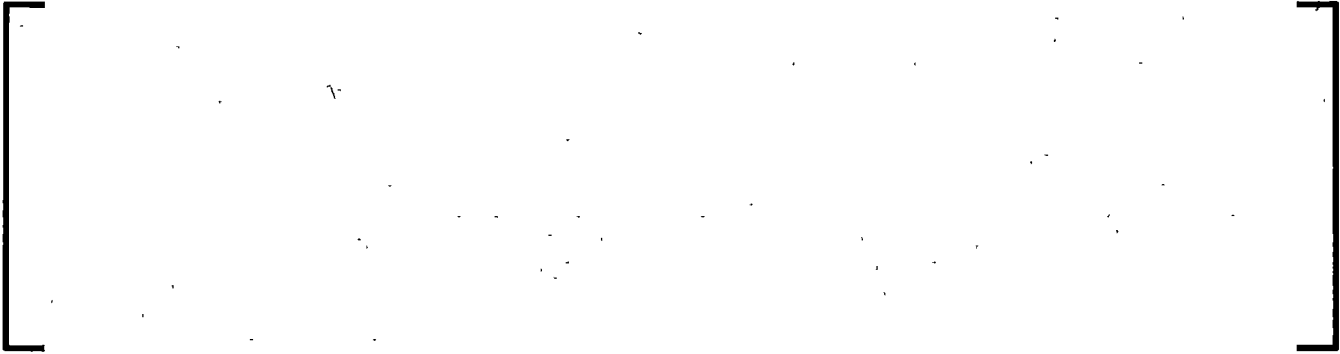
**Figure 2-1 Benchmark Comparison of Impact Force Squared as a
Function of Impact Kinetic Energy, BOL Hot**

Framatome Inc.

ANP-10337 Supplement 1Q2NP
Revision 0

Response to Request for Additional Information - ANP-10337 Supplement 1
Topical Report

Page 2-21

**Figure 2-2 Benchmark Comparison of Total Deformation as a
Function of Impact Kinetic Energy, BOL Hot**

Framatome Inc.

ANP-10337 Supplement 1Q2NP
Revision 0

Response to Request for Additional Information - ANP-10337 Supplement 1
Topical Report

Page 2-22

**Figure 2-3 Benchmark Comparison of Residual Deformation as a
Function of Impact Kinetic Energy, BOL Hot**

**Figure 2-4 Benchmark Comparison of Impact Force as a Function of
Total Deformation, BOL Hot**

Framatome Inc.

ANP-10337 Supplement 1Q2NP
Revision 0

Response to Request for Additional Information - ANP-10337 Supplement 1
Topical Report

Page 2-24

**Figure 2-5 Benchmark Comparison of Restitution Coefficient as a
Function of Impact Kinetic Energy, BOL Hot**

Figure 2-6 Benchmark Comparison of Impact Force Squared as a Function of Impact Kinetic Energy, EOL Cold

**Figure 2-7 Benchmark Comparison of Total Deformation as a
Function of Impact Kinetic Energy, EOL Cold**

Framatome Inc.

ANP-10337 Supplement 1Q2NP
Revision 0

Response to Request for Additional Information - ANP-10337 Supplement 1
Topical Report

Page 2-27

**Figure 2-8 Benchmark Comparison of Residual Deformation as a
Function of Impact Kinetic Energy, EOL Cold**

Framatome Inc.

ANP-10337 Supplement 1Q2NP
Revision 0

Response to Request for Additional Information - ANP-10337 Supplement 1
Topical Report

Page 2-28

Figure 2-9 Benchmark Comparison of Impact Force as a Function of Total Deformation, EOL Cold

Figure 2-10 Benchmark Comparison of Restitution Coefficient as a Function of Impact Kinetic Energy, EOL Cold

Figure 2-11 Reverse Protocol Comparison, Impact Force Squared as a Function of Impact Kinetic Energy, BOL Hot

Framatome Inc.

ANP-10337 Supplement 1Q2NP
Revision 0

Response to Request for Additional Information - ANP-10337 Supplement 1
Topical Report

Page 2-31

Figure 2-12 Reverse Protocol Comparison, Total Deformation as a Function of Impact Kinetic Energy, BOL Hot

Framatome Inc.

ANP-10337 Supplement 1Q2NP
Revision 0

Response to Request for Additional Information - ANP-10337 Supplement 1
Topical Report

Page 2-32

Figure 2-13 Reverse Protocol Comparison, Residual Deformation as a Function of Impact Kinetic Energy, BOL Hot

Figure 2-14 Reverse Protocol Comparison, Restitution Coefficient as a Function of Impact Kinetic Energy, BOL Hot

**Figure 2-15 Reverse Protocol Comparison, Impact Force Squared as
a Function of Impact Kinetic Energy, EOL Cold, Test 1 (Grid 103679)**

**Figure 2-16 Reverse Protocol Comparison, Impact Force Squared as
a Function of Impact Kinetic Energy, EOL Cold, Test 2 (Grid 103680)**

Framatome Inc.

ANP-10337 Supplement 1Q2NP
Revision 0

Response to Request for Additional Information - ANP-10337 Supplement 1
Topical Report
Page 2-36

**Figure 2-17. Reverse Protocol Comparison, Total Deformation as a
Function of Impact Kinetic Energy, EOL Cold, Test 1 (Grid 103679)**

**Figure 2-18 Reverse Protocol Comparison, Total Deformation as a
Function of Impact Kinetic Energy, EOL Cold, Test 2 (Grid 103680)**

Framatome Inc.

ANP-10337 Supplement 1Q2NP
Revision 0

Response to Request for Additional Information - ANP-10337 Supplement 1
Topical Report

Page 2-38

Figure 2-19 Reverse Protocol Comparison, Residual Deformation as a Function of Impact Kinetic Energy, EOL Cold, Test 1 (Grid 103679)

**Figure 2-20 Reverse Protocol Comparison, Residual Deformation as
a Function of Impact Kinetic Energy, EOL Cold, Test 2 (Grid 103680)**

Framatome Inc

ANP-10337 Supplement 1Q2NP
Revision 0

Response to Request for Additional Information - ANP-10337 Supplement 1
Topical Report

Page 2-40

Figure 2-21 Reverse Protocol Comparison, Restitution Coefficient as a Function of Impact Kinetic Energy, EOL Cold, Test 1 (Grid 103679)

Framatome Inc.

Response to Request for Additional Information - ANP-10337 Supplement 1
Topical Report

ANP-10337 Supplement 1Q2NP
Revision 0

Page 2-41

Figure 2-22 Reverse Protocol Comparison, Restitution Coefficient as a Function of Impact Kinetic Energy, EOL Cold, Test 2 (Grid 103680)

Framatome Inc

ANP-10337 Supplement 1Q2NP

Revision 0

Response to Request for Additional Information - ANP-10337 Supplement 1

Topical Report

Page 2-42

Figure 2-23 Random Protocol Comparison, Impact Force as a Function of Impact Number, BOL Hot

**Figure 2-24 Random Protocol Comparison, Residual Deformation as
a Function of Impact Number, BOL Hot**

**Figure 2-25 Random Protocol Comparison, Impact Force as a
Function of Impact Number, EOL Cold**

**Figure 2-26 Random Protocol Comparison, Residual Deformation as
a Function of Impact Number, EOL Cold**

Framatome Inc.

Response to Request for Additional Information - ANP-10337 Supplement 1
Topical Report

ANP-10337 Supplement 1Q2NP
Revision 0

Page 3-1

3.0   RAI 6

Question:

The topical report primarily discusses two-sided impact behavior. Provide a discussion of any data related to how the example grid from Supplement 1 to ANP-10337 would behave under one-sided impacts, including how any deformation is distributed along the grid in both directions. Discuss how the acceptance criteria for maximum allowable deformation, including the approach discussed in the topical report of adding two half deformations from adjacent DGEs, is consistent with the underlying thermal hydraulic

Response:

The RAI 6 question has two parts:

1. Discussion of any data related to how the example grid of Supplement 1 to ANP-10337 behaves under one-sided impacts, including how any deformation is distributed along the grid in both directions.

2. Discussion of the consistency between the deformation acceptance criteria in Supplement 1 (including the approach of adding two half deformations from adjacent grids) and the underlying thermo-hydraulic and control rod insertability requirements when considering the one-sided deformation pattern. The specific issue is that the acceptance criteria may implicitly allow local deformation beyond that which is supported by thermo-hydraulic and insertability evaluations.

The response is organized along the lines of the RAI question itself. In the first part of the response the data related to other types of grid loading is presented, and in the second part the very conservative character of the proposed Deformable Grid Element (DGE), its current test basis, and acceptability of modeling one-sided impacts with a uniform deformation model are discussed. Along with the discussion of the second part of RAI 6, a change in the methodology defined in Section 5.2 of Supplement 1 to ANP-10337P-A (Reference 1) is described. The change entails reporting the residual deformation for half grid segments rather than the sum of two half grid segments.

As a consequence, the allowable deformation for a half grid segment is half of the allowable deformation defined in Section 3.2 of Supplement 1 to ANP-10337P-A (Reference 1), and Section 4 of ANP-10337P-A (Reference 3).

TEST RESULTS FROM OTHER TYPES OF GRID LOADING

Framatome has performed grid tests in [   ] for several grid designs. The standard spacer grid testing protocol for Framatome is the [

                                                          ] tested on a dynamic impact bench as discussed in Section 6 of Reference 3.

The test approach described in this section [

] In this configuration it is possible to perform tests [

] The test arrangement is shown in Figure 3-1.

The second configuration [

] The test arrangement is shown in Figure 3-2.

A total number of [

]

Framatome Inc.

Response to Request for Additional Information - ANP-10337 Supplement 1
Topical Report

ANP-10337 Supplement 1Q2NP
Revision 0

Page 3-4

At the end of the tests, one grid [

] and the deformation

was measured on a Coordinate Measurement Machine (CMM) to provide a more

detailed assessment of the permanent deformation pattern.

The results from the [

] tests, which form the basis for the sample problem of the

Deformable Grid Element (reference 1), and support the following observations:

[

]

Framatome Inc.

ANP-10337 Supplement 1Q2NP
Revision 0

Response to Request for Additional Information - ANP-10337 Supplement 1
Topical Report

Page 3-5

[

]
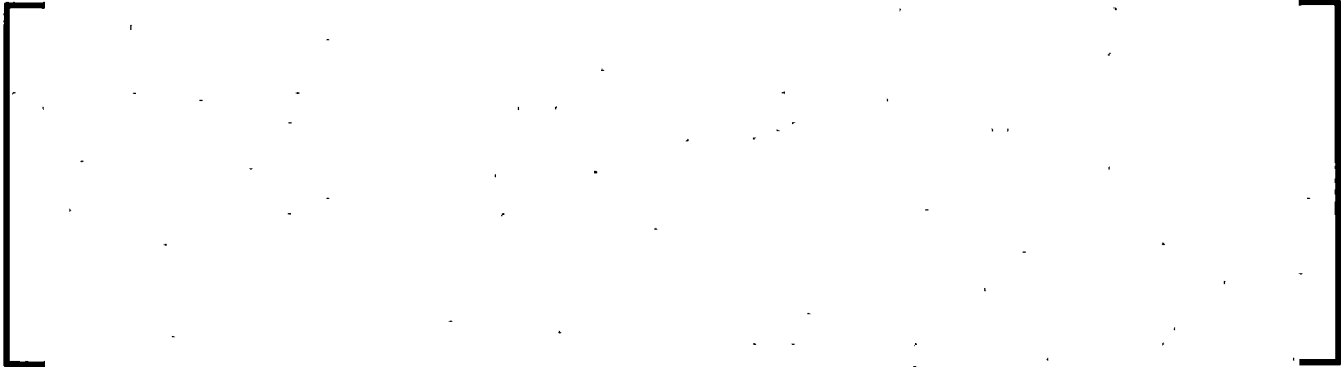
Since the DGE acceptance criterion is based on the residual grid deformation

(reference 1), a comparison of [

] permanent grid deformation is shown in Figure 3-3. Comparing the two sets

of data it is apparent that for the same level of [

]

Another important aspect of the accumulated permanent grid deformation is the uniform

distribution throughout the grid. The CMM data for the [

] which form the basis for the DGE grid models.

The results from the [

]

Given that the acceptance criterion for the DGE is the accumulated grid permanent

deformation, a comparison of the [

            ] in terms of grid deformation is shown in Figure 3-6, which reproduces the

data in Figure 3-3, and adds the [

      ]   The data supports a few observations and conclusions as follows:

Framatome Inc.

Response to Request for Additional Information - ANP-10337 Supplement 1
Topical Report

ANP-10337 Supplement 1Q2NP
Revision 0

Page 3-8

[

]

The other important aspect of the [

] direction is approximately zero.

However as discussed above, this deformation [

] tests and it is applied to all impacts regardless of
their type. A more detailed discussion on this point is presented in the next section.

Framatome Inc.

ANP-10337 Supplement 1Q2NP
Revision 0

Response to Request for Additional Information - ANP-10337 Supplement 1
Topical Report

Page 3-9

SUITABILITY OF THE DGE MODEL FOR ALL LOADING SCENARIOS

The second part of RAI #6 question is with respect to the possibility that the half-element DGE, being derived from the full-element DGE by [

]

The suitability of the DGE grid model for this scenario rests on the [

]

[

]

Therefore, using the deformation prediction of the DGE for all types of impacts [

]

In order to get a more accurate representation of predicted permanent deformation levels from the core row model, a change in the margin reporting is implemented in the sample problem. The permanent deformation of the baffle plate to fuel assembly half-grid elements is reported, and is compared to [

] acceptable deformation.

Supplement 1 to ANP-10337 (Reference 1) will be changed to reflect this revised approach. A markup of Section 5.2 of Reference 1 is included in Section 9 of this document.

Figure 3-1 [**] Configuration – Actual Hardware**

Figure 3-2 [   ] Configuration – Actual Hardware

Framatome Inc.

ANP-10337 Supplement 1Q2NP
Revision 0

Response to Request for Additional Information - ANP-10337 Supplement 1
Topical Report

Page 3-13

Figure 3-3 [   ] Grid
Permanent Deformation

Framatome Inc

ANP-10337 Supplement 1Q2NP
Revision 0

Response to Request for Additional Information - ANP-10337 Supplement 1
Topical Report

Page 3-14

Figure 3-4 [   ] Grid Test – Deformation Distribution

[

Framatome Inc.

ANP-10337 Supplement 1Q2NP
Revision 0

Response to Request for Additional Information - ANP-10337 Supplement 1
Topical Report

Page 3-15

Figure 3-5 [ ] Grid Test
Results

[

]

Framatome Inc.

ANP-10337 Supplement 1Q2NP
Revision 0

Response to Request for Additional Information - ANP-10337 Supplement 1
Topical Report

Page 3-16

Figure 3-6 [   ] **Grid Permanent Deformation**

Framatome Inc.

ANP-10337 Supplement 1Q2NP
Revision 0

Response to Request for Additional Information - ANP-10337 Supplement 1
Topical Report

Page 3-17

Figure 3-7 [**] Grid Permanent Deformation Distribution**

Framatome Inc

Response to Request for Additional Information - ANP-10337 Supplement 1
Topical Report

ANP-10337 Supplement 1Q2NP
Revision 0

Page 4-1

4.0   RAI 7

Question:

Identify and describe the primary and secondary stresses that affect the guide tubes and fuel rods in a Supplement 1 analysis. Also explain why the ANP-10337 control rod insertion test database and control rod insertion acceptance criteria remains applicable to Supplement 1 analyses that include the DGE.

Response:

PRIMARY AND SECONDARY STRESSES IN FUEL RODS AND GUIDE TUBES IN THE PRESENCE OF GRID DEFORMATION

The fuel assembly component stress classification and acceptance criteria for the fuel designs equipped with deformable grid elements (Reference 1) are the same as the ones for fuel designs with visco-elastic grid elements (Reference 3), for all sources of stress which are common to both cases. For the DGE, there is [

] in the

direction of impact. The ANP-10337P-A Supplement 1 (Reference 1). [

] per the terminology of the ASME Code Section III. A brief discussion to clarify the appropriateness of this classification is contained in the subsequent paragraphs.

Section III of the ASME Code (NB-3213.9) defines secondary stresses as:

> *Secondary stress is a normal stress or a shear **stress developed by the constraint of adjacent material or by self-constraint of the structure**. The basic characteristic of a secondary stress is that it is self-limiting. Local yielding and minor distortions can satisfy the conditions that cause the stress to occur and failure from one application of the stress is not to be expected.*

By contrast, the primary stress is defined in NB-3213.8 as:

> *Primary stress is any normal stress or shear stress developed by an imposed*
> *loading that is **necessary to satisfy the laws of equilibrium of external and***
> ***internal forces and moments.** The basic characteristic of a primary stress is*
> *that it is not self-limiting. Primary stresses that considerably exceed the yield*
> *strength will result in failure or, at least, in gross distortion.*

The essential difference between primary and secondary stress is that primary stresses are necessary to maintain equilibrium with external loads, while secondary stresses are present due to the self-constraint of the structure, and are associated with an imposed strain pattern. To illustrate this point, consider the case of a beam on pinned supports (Figure 4-1-A). In this case the external force F_{ext} creates a displacement δ and a state of stress which is **necessary to maintain the equilibrium** with the applied external force. This stress is not equilibrating within the structure, nor is it self-limiting. If the external force increases, the stress has to increase as well in order to maintain equilibrium, and if the beam material yields though the section, the structure collapses. This case illustrates a typical primary stress. In Figure 4-1-B, the structure is composed of two beams and the same displacement δ is applied in opposite directions by a restraining device. In this case the beams experience the same state of stress as in case A, but these stresses are equilibrating within the structure. The structure is in equilibrium under zero external force, hence these stresses are not needed to maintain equilibrium with external forces, but arise from the self-constraint of the structure, which is forced to comply with an imposed displacement pattern. This case illustrates a typical secondary stress.

The considerations from the example above [

]

The ASME Code defines different types of limits for primary and secondary stress. The primary stresses are controlled by the *Pm* and *Pm+Pb* limits, while the secondary stresses are controlled by the *3Sm* criterion on the primary plus secondary stress intensity range. Secondary stresses also must be taken into account in buckling evaluations. This design philosophy relies on the capability of the material to redistribute stress by localized yielding, by assuming sufficient levels of ductility. The fuel cladding and guide tube materials discussed in ANP-10337P-A (Reference 3, RAI-20, Appendix B and Appendix D) have a substantial total ultimate elongation even in the irradiated condition, which justifies the application of the methods of the ASME Code.

As a further confirmation [

] and therefore retain their

validity.

As mentioned previously, secondary stresses must be taken into account for the buckling evaluation. In the DGE Supplement (Reference 1) these stresses [

]

ACCEPTABILITY OF DGE IMPOSED FUEL ROD AND GUIDE TUBE DEFLECTIONS RELATIVE TO CONTROL ROD INSERTION ASSESSMENT

The DGE deformation resulting in additional guide tube bending raises the question of the adequacy of the control rod insertion test data base used to support the Level C acceptance criteria for the guide tubes (Reference 3, Appendix F), especially since the bending stress associated with this deflection is classified as secondary, and therefore not included in the Level C stress criteria.

The analyzed scenarios in the sample problem for the DGE Supplement (reference 1) include very conservative levels of seismic and LOCA loads, in order to exercise the DGE to high levels of deformation. The cumulative grid permanent deformations under the Design Basis Accident (DBA) are calculated as a combination of seismic and LOCA, with sensitivity penalties applied. The results show that the controlling case [

]

[   ] does not make a meaningful

difference. For the mode 3 deformations, it is worth pointing out that the grid permanent

deformations are [

                                                                                          ] it can be concluded

that the arguments of the RAI 20 response remain valid, and that the DGE does not

pose additional challenges to the use of Level C limits (together with buckling) to

ascertain control rod insertion.

Framatome Inc.

ANP-10337 Supplement 1Q2NP
Revision 0

Response to Request for Additional Information - ANP-10337 Supplement 1
Topical Report

Page 4-6

Figure 4-1 Illustration of Primary and Secondary Stress

$$F_{ext} > 0 \qquad \delta$$

[A]

$$F_{ext} = 0 \qquad \delta$$

[B]
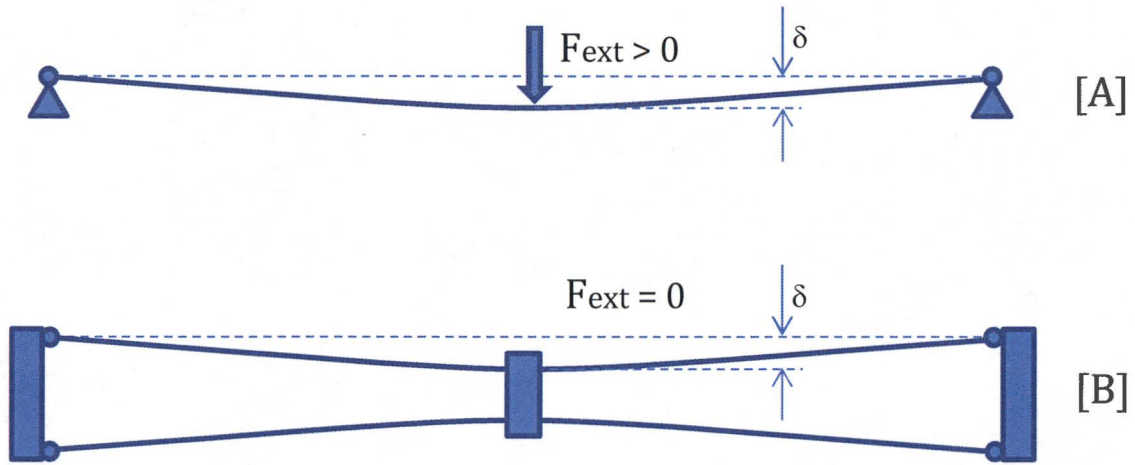
5.0   RAI 9

Question:

Irradiation has a known effect of causing materials to harden (irradiation hardening). This would be expected to affect the response of deformable spacer grid designs, since their energy absorption properties as a function of impact load would be expected to change. This may affect: (1) how much energy the spacer grid can absorb before failure, and (2) how much energy the spacer grid would pass along to the next spacer grid element in the row. Discuss how any potential non-conservatisms from this change in behavior would be accommodated in the analysis methodology, including failure of the grid in question or one of its neighboring grids in the seismic analysis.

Response:

The irradiation hardening of the spacer grid material is addressed in the EOL impact test protocol, where the test is [

                                                                                            ]

It is important to note that the spacer grid deformation mode does not change when tested in [   ] The [   ] is maintained due to the design and construction of the spacer grids for which the DGE is applicable. Therefore, failure for a spacer grid with [   ] must be defined in terms of a residual deformation limit.

Also, as discussed in Appendix D of Reference 3, [

                                                ] Therefore, the total effect of irradiation

hardening is to increase the energy the spacer grid can absorb before reaching the

residual deformation limit. In this respect the EOL impact test protocol is conservative.

Again, the failure mode of the spacer grid is not expected to change since this behavior

is controlled by the construction of the spacer grid.

A potential non-conservatism is the interaction between a fully hardened spacer grid

and a partially hardened spacer grid (one with less exposure). [

        ] The potential non-conservatism also relies on having two adjacent spacer

grids with different degrees of irradiation hardening. In this case the spacer grid with

more irradiation hardening would absorb less of the impact kinetic energy, resulting in

less residual deformation, and instead concentrate the residual deformation in the

adjacent spacer grid with less irradiation hardening. If the two adjacent spacer grids

were either in the fully BOL condition or the fully EOL condition, then the energy

exchange of impacting and rebounding kinetic energy would be balanced.

Two aspects of the deformable grid methodology must be adjusted as a result of this

RAI response.

First, Section 5.1.2 of the Supplement will be revised to explicitly state that the situation
where two adjacent spacer grids have different energy absorption characteristics

[

                                                                              ] Thus, it

can be demonstrated that the potential non-conservatism of under estimating the

energy absorption properties of a fully hardened spacer grid can be treated in a

conservative manner.

As an example, consider that a BOL GAIA assembly is adjacent to an EOL GAIA

assembly.   [

                                              ]

Framatome Inc.

ANP-10337 Supplement 1Q2NP
Revision 0

Response to Request for Additional Information - ANP-10337 Supplement 1
Topical Report

Page 5-4
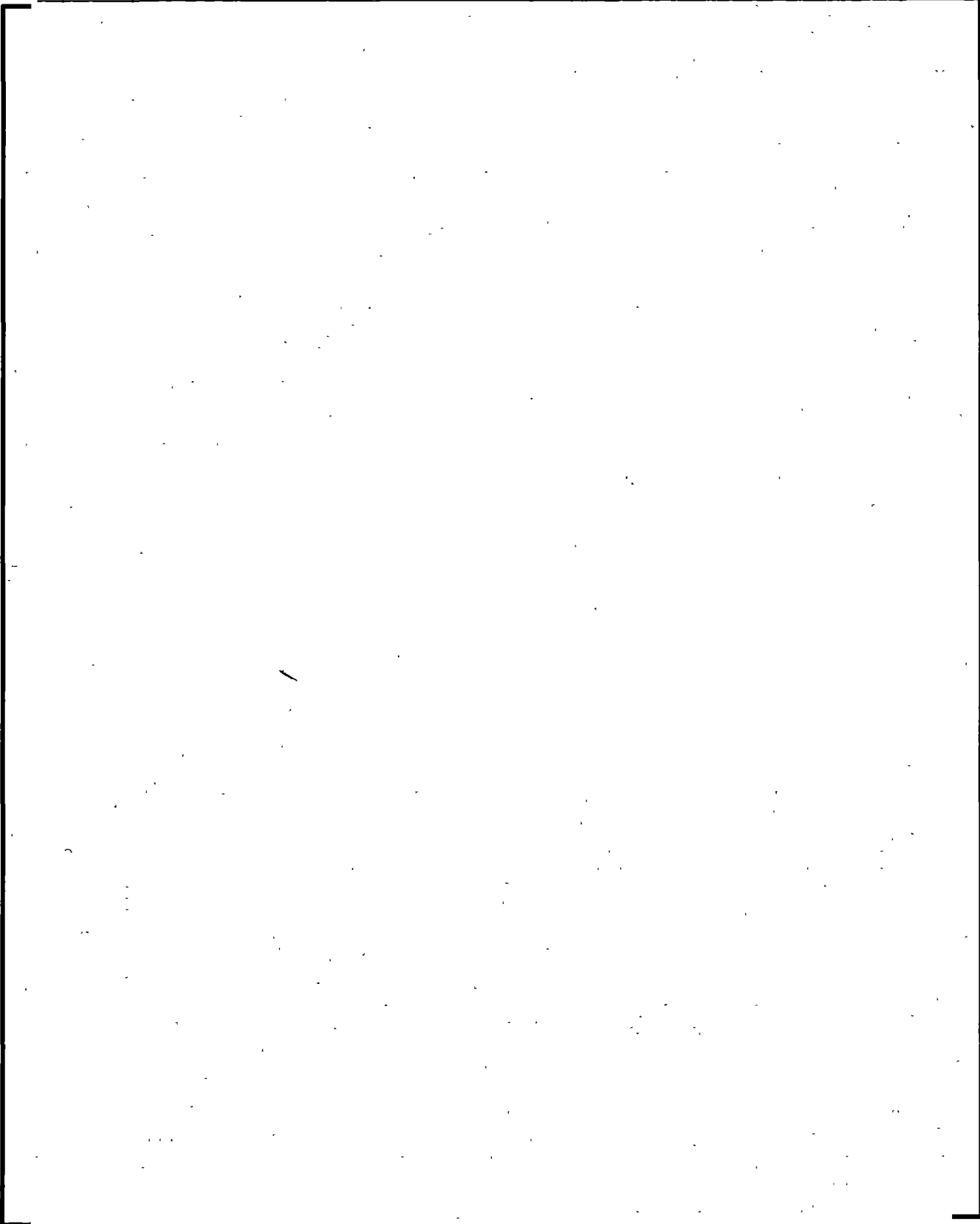
Table 5-1: Residual Deformation for BOL and Mixed BOL / EOL Row Configurations

	Full BOL [mm]	Mix (A/B) BOL-EOL [mm]
SSE-Z (9 FA's)	0.247	0.434 / 0.339
ACC-Z (3 FA's)	0.701	0.771

Figure 5-1: BOL and Mixed BOL / EOL Row Configurations

| BOL | EOL | BOL |

3 Assemblies Row

| BOL | EOL | EOL | EOL | EOL | EOL | EOL | EOL | BOL |

9 Assemblies Row - Option A

| EOL | BOL | EOL | EOL | EOL | EOL | EOL | BOL | EOL |

9 Assemblies Row - Option B

Framatome Inc.

ANP-10337 Supplement 1Q2NP
Revision 0

Response to Request for Additional Information - ANP-10337 Supplement 1
Topical Report

Page 6-1

6.0   RAI 10

Question:

In many pressurized water reactor core designs, some fresh fuel assemblies may be loaded with one corner on the core periphery. This exposes the fuel to a very steep flux gradient, which produces a significant exposure tilt across the fuel assembly. Discuss whether the non-uniform irradiation hardening would lead to non-uniform deformation behavior across the grid, thus violating one of the criteria for use of the DGE.

Response:

It is possible that a fresh fuel assembly can be loaded with one corner on the core periphery. [

] Fuel assemblies that do experience a high flux gradient (or burnup gradient) are subject to further core shuffle design constraints.

The non-uniform irradiation hardening is not anticipated to produce a non-uniform deformation behavior across the spacer grid. It is important to clarify the definition of uniform deformation for this response. [

] A non-uniform deformation would be a concentration of deformation in a small number of rows. The typical example of a non-uniform deformation is shear racking. This deformation mode is illustrated in Figure 10-1. In this case a 2 mm residual deformation results in a large transverse displacement of several guide tube rows as well as a significant reduction of the flow areas. The shear racking also signifies the collapse and loss of load-carrying capacity of the grid. It is this behavior that is to be avoided in a deformable grid methodology.

Framatome Inc.

Response to Request for Additional Information - ANP-10337 Supplement 1
Topical Report

ANP-10337 Supplement 1Q2NP
Revision 0
Page 6-2

The uniform deformation of the GAIA spacer grid is directly attributable to the design. The spring hulls at the inner strip intersections prevent the sudden loss of load-carrying capacity and shear racking deformation. The benefit is substantiated by comparing beginning of life (BOL) and end of life (EOL) impact tests. Spacer grids designs like the HTP grid transition from a uniform deformation (pre-buckling) in BOL conditions to a non-uniform deformation in EOL conditions with the loss of the cladding-grid spring preload. The GAIA spacer grid, however, maintains the same uniform deformation and load-carrying capacity in EOL conditions as in BOL conditions.

A uniform deformation behavior does not require that the residual deformation be exactly distributed across each fuel rod pitch. Data presented in Figure A-21 and A-22 from Reference 4 (reproduced as Figure 10-2 and Figure 10-3 below) shows non-negligible deviations from the theoretical decrease in pitch across the envelope of a BOL HTP spacer grid. The BOL HTP spacer grid demonstrates a high degree of uniform deformation prior the peak impact load. The variation in pitch between rows can be attributed to any number of parameters such as guide tube positions, weld nugget size, or manufacturing imperfections. These variations do not negatively impact the RCCA insertion or the thermal-hydraulic justification.

A study was performed to estimate the effects of a flux gradient on the deformation

behavior of a GAIA spacer grid. A neutronics calculation determined the flux gradient

for four locations on the core periphery. The largest flux gradient, [

                                                                ] was used as input to calculate

the difference in yield strength as a function of fluence and position in the spacer grid.

[

]

Framatome Inc.

ANP-10337 Supplement 1Q2NP
Revision 0

Response to Request for Additional Information - ANP-10337 Supplement 1
Topical Report

Page 6-4

Figure 6-1 Example Spacer Grid with Non-uniform Deformation
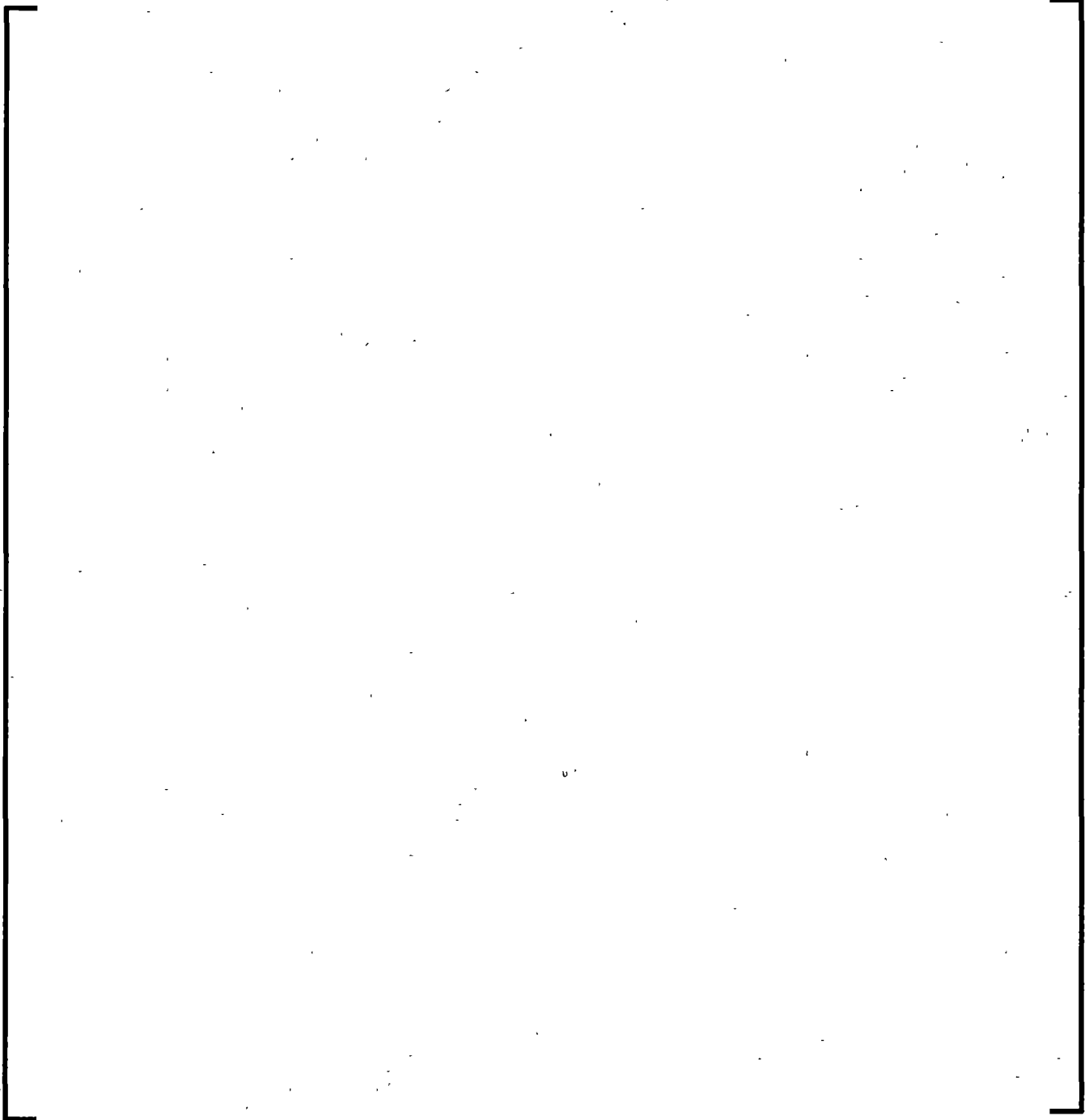
Figure 6-2 Spacer Grid B30121 – Cumulative and Individual Fuel Rod Pitch Data

Framatome Inc.

ANP-10337 Supplement 1Q2NP
Revision 0

Response to Request for Additional Information - ANP-10337 Supplement 1
Topical Report

Page 6-6

Figure 6-3 Spacer Grid B30122 – Cumulative and Individual Fuel Rod Pitch Data

7.0   ADDITIONAL INFORMATION

The sample problem spacer grid benchmark analysis and lateral seismic / LOCA analysis were revised to correct the error in the equation for the calculated F-statistic. This error was identified in the previously submitted RAI responses. Appendix B of the Supplement has been updated with the results of the revised spacer grid benchmark. Appendix C of the supplement has been updated with the results of the lateral seismic / LOCA analysis using the updated DGE input parameters. The results of Appendix C also include the change in residual deformation post-processing described in RAI 9.

Change pages to ANP-10337 Supplement 1 are provided in Section 9 of this document.

Framatome Inc.

ANP-10337 Supplement 1Q2NP
Revision 0

Response to Request for Additional Information - ANP-10337 Supplement 1
Topical Report

Page 8-1

8.0   REFERENCES

1. ANP-10337P-A, Revision 0, Supplement1P, Revision 0, "Deformable Spacer Grid Element", September 2018.

2. Letter, Jonathan Rowley (NRC) to Gary Peters (Framatome Inc.), "Request for Additional Information Related to Topical Report ANP-10337P, Revision 0, Supplement 1P, Revision 0 "Deformable Spacer Grid Element" Framatome, Inc. (EPID: L-2018-TOP-0037), May 15, 2019.

3. ANP-10337P-A, Revision 0, PWR Fuel Assembly Structural Response to Externally Applied Dynamic Excitations

4. ANP-10325P, Revision 0, U.S. EPR Fuel Assembly – Faulted Condition Analysis

9.0   MARKUP PAGES

Framatome Inc.

Deformable Spacer Grid Element
Topical Report

ANP-10337
Revision 0
Supplement 1NP
Revision 0
Page 4-10

The regressions calculated per Section 4.6.1 are used to develop a target behavior to

be matched by the output of the deformable grid element.   [

]

Framatome Inc.

Deformable Spacer Grid Element
Topical Report

ANP-10337
Revision 0
Supplement 1NP
Revision 0
Page 5-2

5.1.2   Mixed Core Configurations

In the case of mixed core configurations where the fuel assembly with deformable spacer grids is adjacent to a dissimilar fuel assembly design with linear spacer grids, the DGE must account for the stiffness and damping properties of the adjacent assembly.

The typical mixed core configuration arises when Framatome fuel operates next to fuel from other vendors.

The half deformable grid element and the adjacent linear impact spring are modeled as springs in series.

Framatome Inc.

ANP-10337
Revision 0
Supplement 1NP
Deformable Spacer Grid Element
Topical Report
Revision 0
Page 5-5

5.2   *Processing Deformation Results*

The horizontal row model defined in Section 5.2.2.2 of Reference 1 is unchanged by the introduction of the deformable grid element. Therefore, no single impact element is associated with a single full spacer grid. Instead, the two springs representing a half grid of neighboring assemblies are replaced with a single spring. The desired output of the row model with the deformable grid element is the residual deformation of a spacer grid for a given fuel assembly.

Framatome Inc.

Deformable Spacer Grid Element
Topical Report

ANP-10337
Revision 0
Supplement 1NP
Revision 0
Page 5-6
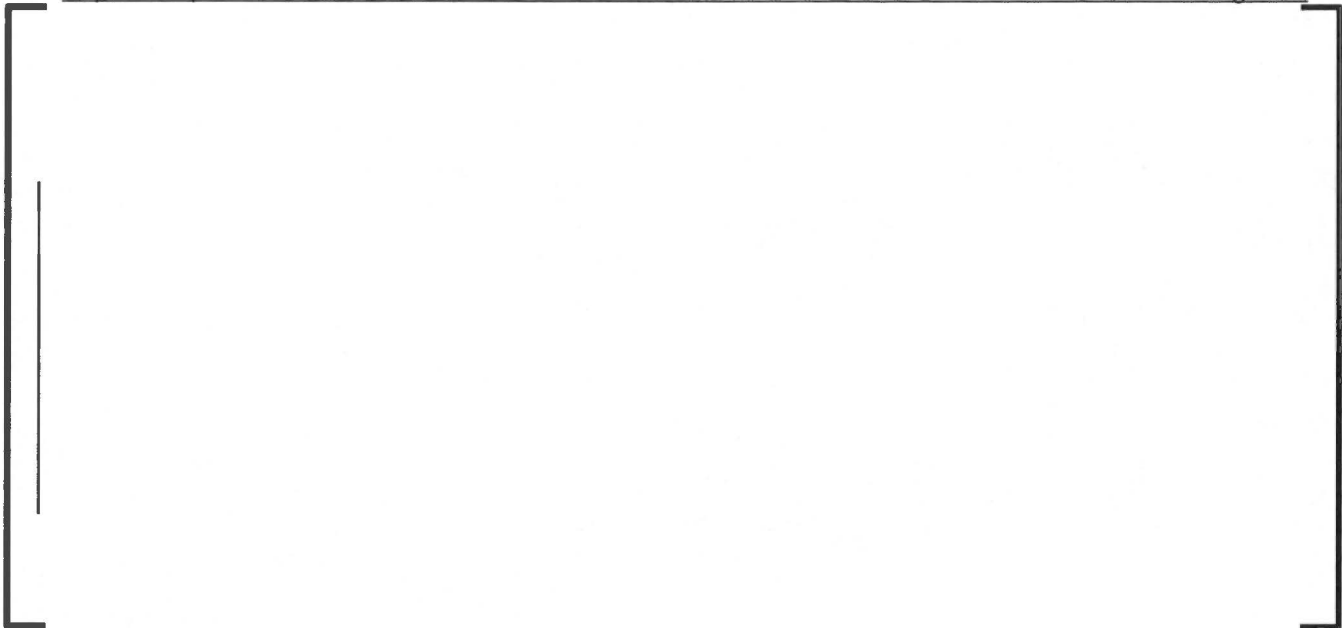
5.3   *SSE + LOCA Combination*

The spacer grid residual deformations from the worst-case LOCA break and the SSE are combined to determine a residual deformation for the Design Basis Accident. This combination is performed to demonstrate conservatism and satisfy the requirements of GDC 2, but it does not reflect any inter-dependency between the two events. Therefore, the SSE and LOCA events are analyzed separately.

The combination of the SSE and LOCA residual deformations is performed by [

]

Framatome Inc.

Deformable Spacer Grid Element
Topical Report

ANP-10337
Revision 0
Supplement 1NP
Revision 0
Page 5-8

5.4 *Experimental Uncertainty and 95% Confidence Limit*

Based on the discussion in Section 4.6, the deformable grid element is benchmarked to

[

] To meet the intent of
the regulatory guidelines of~~comply with the requirements of~~ SRP 4.2, a 95% upper
confidence limit ~~must be~~on the mean response is calculated based on the variability of
the experimental data. The 95% upper confidence limit for a multivariable regression is
calculated from the following equation:

$$Y_{95\ UCL} = Y_{pred} + t_{n-k-1,95\%}\sqrt{MSresX_0^T(X^TX)^{-1}X_0}$$

Where Y_{pred} is the expected value predicted by the regression at X_0,

t_{n-k-1}, 95% is the critical value of the t-distribution for n-k-1 degrees of freedom and a
95% confidence interval,

X_0 is the matrix of desired regressors,

X is the model matrix containing the experimental data,

MSres is the mean squared residual from the regression of the experimental data.

The matrix of desired regressors, X_0, can be found by [

] Then, the 95% upper confidence of the regression at that
particular X_0 can be calculated.

If a sensitivity factor, as defined in SRP 4.2 Appendix A.II.3, is needed for the residual
deformation, then the Ypred in the calculation of the 95% upper confidence limit shall
include the necessary sensitivity factor.

Framatome Inc.

Deformable Spacer Grid Element
Topical Report

ANP-10337
Revision 0
Supplement 1NP
Revision 0
Page B-2

An examination of the experimental data in Figure B-1 indicates that the [

]

The values for Zi are calculated for each experimental data point, and a linear regression is performed to calculate the coefficients, ai. ~~The same values of~~ [

] are shown in Figure B-1 through Figure B-3.

[

]

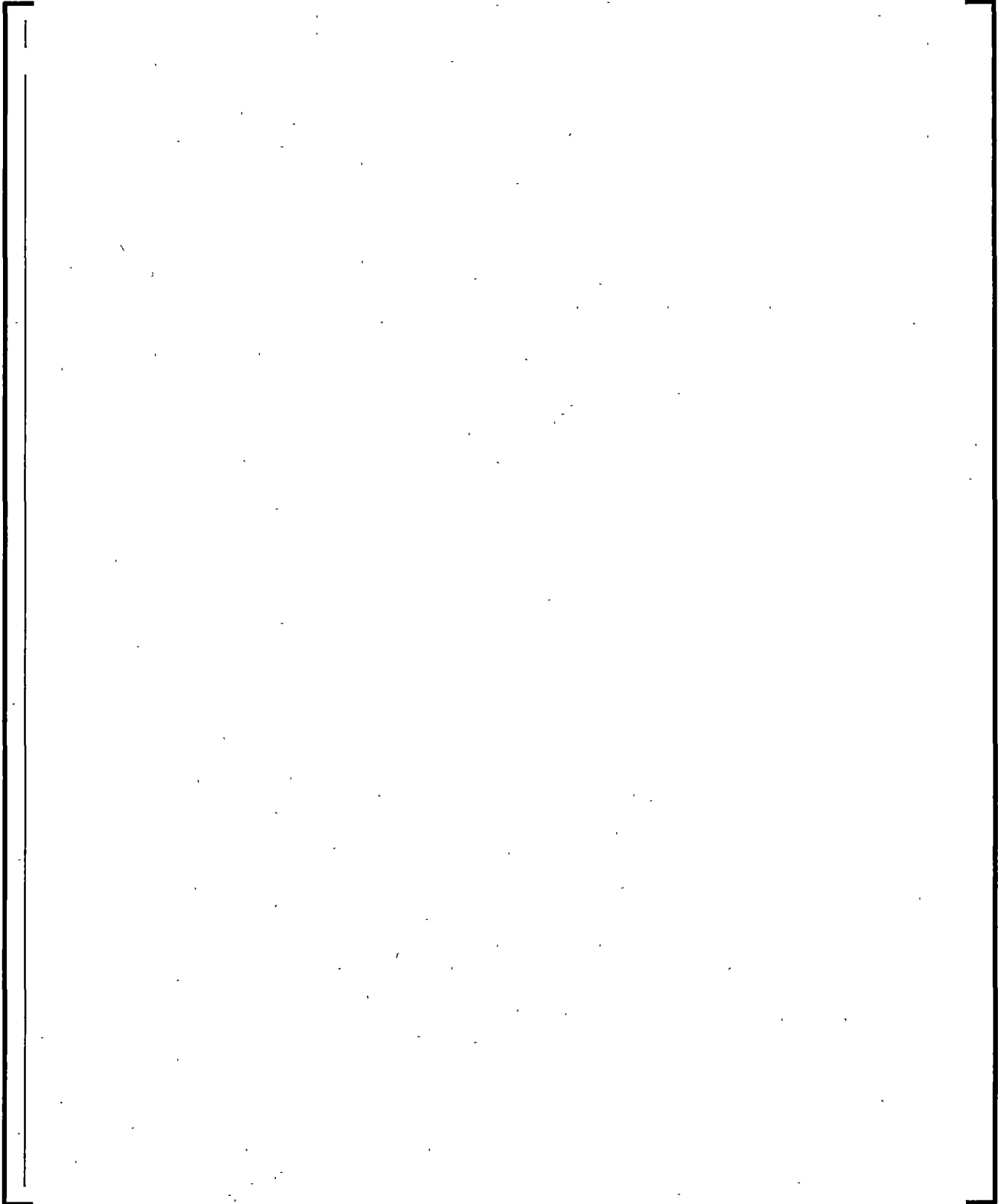## B.3   Adjustment of the Deformable Grid Element Input Parameters

There is no single method for setting the values for the deformable grid element input parameters. Instead, engineering judgement is used to decide how each input parameter should be adjusted to match the target behavior.

Framatome Inc.

Deformable Spacer Grid Element
Topical Report

ANP-10337
Revision 0
Supplement 1NP
Revision 0
Page B-8

[

]

With regards to the benchmarking of the CASAC deformable grid element, the analysis of covariance is performed for the [

] A summary of the ANCOVA results for the example benchmark is provided in Table B-3. The coefficients of determination for the full model regressions are provided in Table B-4. The root mean squared errors of the full model regressions are provided in Table B-5.

The conclusion of the analysis of covariance for the example benchmark is that the difference between the CASAC model output and the experimental data is not statistically significant.

Framatome Inc.

Deformable Spacer Grid Element
Topical Report

ANP-10337
Revision 0
Supplement 1NP
Revision 0
Page B-9

Table B-1: Target Behavior for Deformable Grid Element Benchmark

Framatome Inc.

Deformable Spacer Grid Element
Topical Report

ANP-10337
Revision 0
Supplement 1NP
Revision 0
Page B-10

Table B-2: Deformable Grid Element Input Parameters

[

]

Framatome Inc

Deformable Spacer Grid Element
Topical Report

ANP-10337
Revision 0
Supplement 1NP
Revision 0
Page B-11

Table B-3: BOL Analysis of Covariance Results

$$\Bigg[\hspace{12cm} \Bigg]$$

Table B-4: Coefficients of Determination

$$\Bigg[\hspace{12cm} \Bigg]$$

Table B-5: Root Mean Squared Error

$$\Bigg[\hspace{12cm} \Bigg]$$

Framatome Inc.

Deformable Spacer Grid Element
Topical Report

ANP-10337
Revision 0
Supplement 1NP
Revision 0
Page B-12

Figure B-1: Regression of [
] BOL

Framatome Inc.

ANP-10337
Revision 0
Supplement 1NP
Revision 0

Deformable Spacer Grid Element
Topical Report
Page B-13

Figure B-2: Regression of [

] BOL

[

]

Framatome Inc.

·ANP-10337
Revision 0
Supplement 1NP
Revision 0
Page B-14

Deformable Spacer Grid Element
Topical Report

Figure B-3: Regression of [

] BOL

Framatome Inc

Deformable Spacer Grid Element
Topical Report

ANP-10337
Revision 0
Supplement 1NP
Revision 0
Page B-15

Figure B-4: Benchmark Comparison of Impact Force Squared as a Function of Kinetic Energy, BOL Hot

Framatome Inc.

Deformable Spacer Grid Element
Topical Report

ANP-10337
Revision 0
Supplement 1NP
Revision 0
Page B-16

**Figure B-5: Benchmark Comparison of Total Deformation as a
Function of Kinetic Energy, BOL Hot**

Framatome Inc.

Deformable Spacer Grid Element
Topical Report

ANP-10337
Revision 0
Supplement 1NP
Revision 0
Page B-17

Figure B-6: Benchmark Comparison of Impact Force as a Function of Total Deformation, BOL Hot

Framatome Inc.

ANP-10337
Revision 0
Supplement 1NP
Revision 0
Page B-18

Deformable Spacer Grid Element
Topical Report

Figure B-7: Benchmark Comparison of Residual Deformation as a Function of Kinetic Energy, BOL Hot

Framatome Inc.

ANP-10337
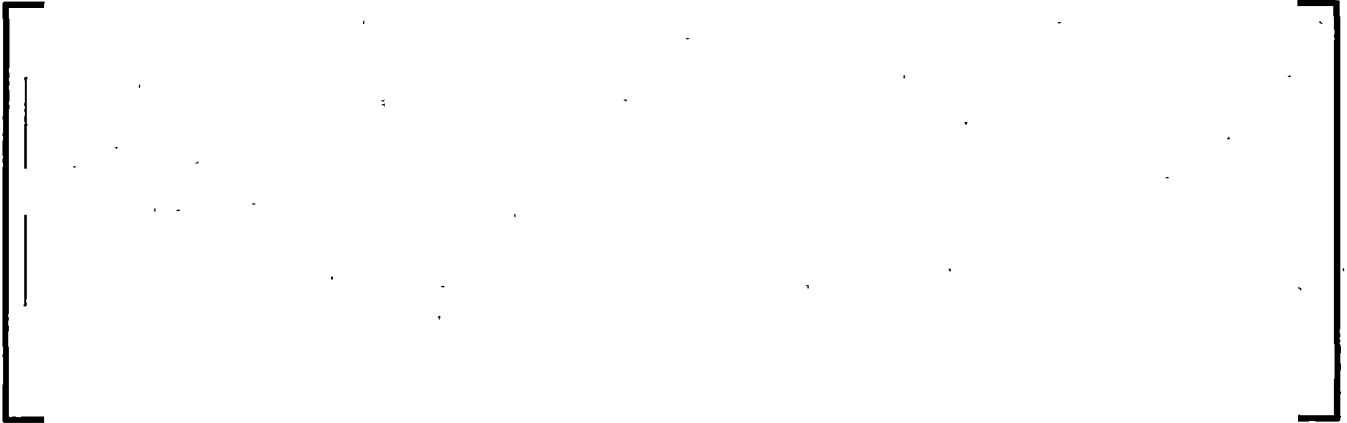Revision 0
Supplement 1NP
Deformable Spacer Grid Element
Revision 0
Topical Report
Page B-19
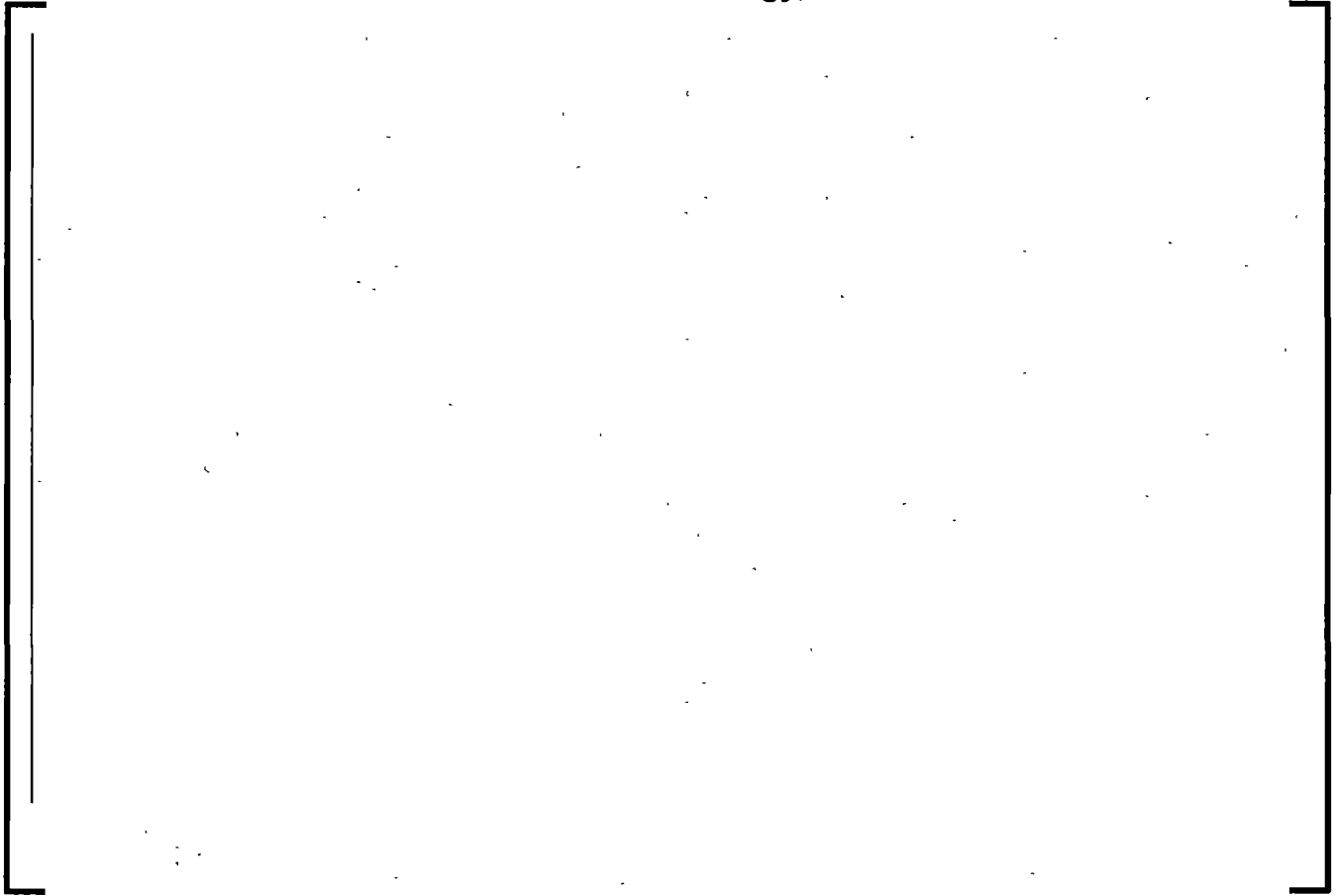
**Figure B-8: Benchmark Comparison of Restitution Coefficient as a
Function of Kinetic Energy, BOL Hot**

Framatome Inc.

ANP-10337
Revision 0
Supplement 1NP
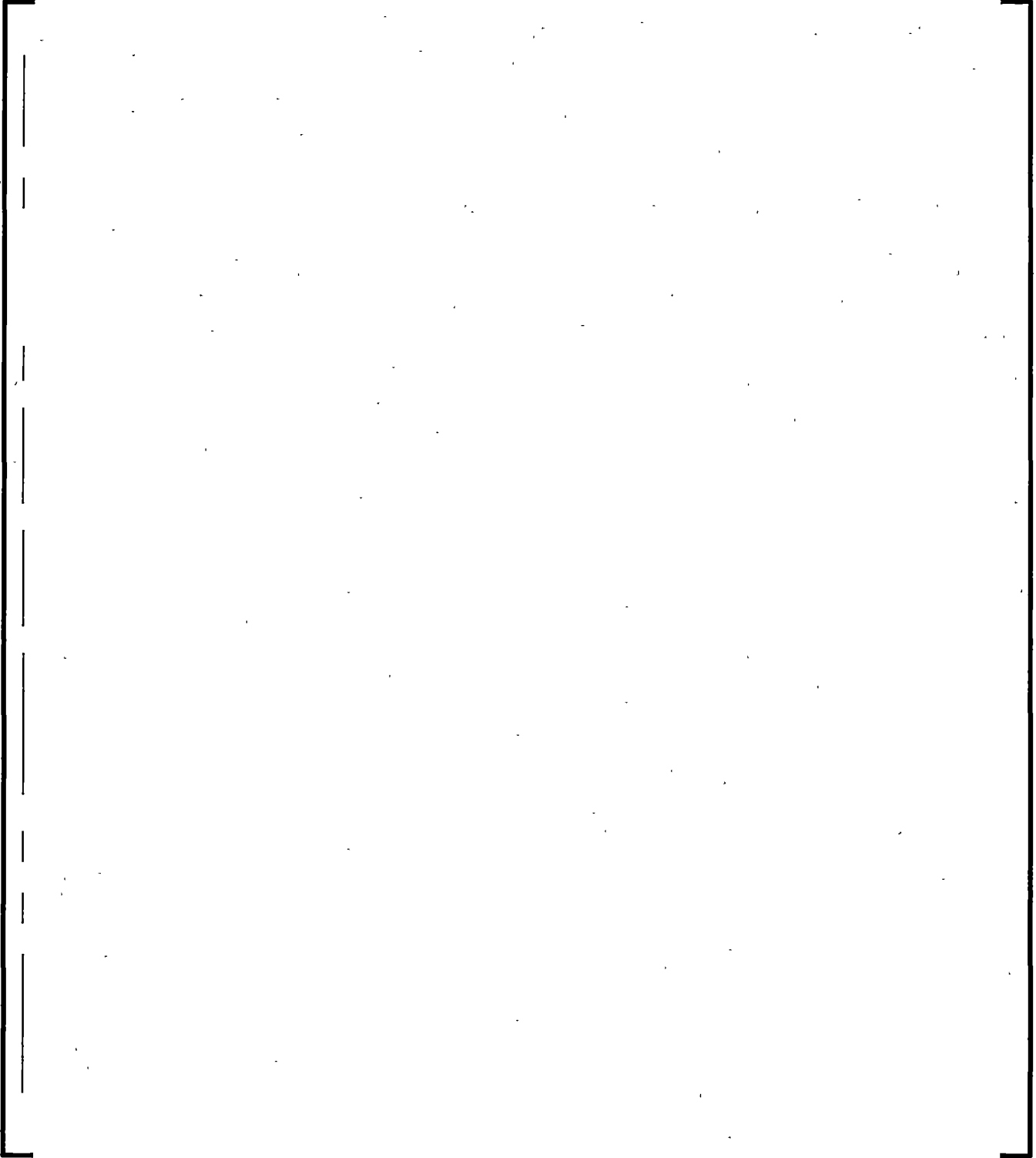Deformable Spacer Grid Element
Revision 0
Topical Report
Page C-11

Table C-4: Rotational Stiffness Values at Operating Conditions

[

]
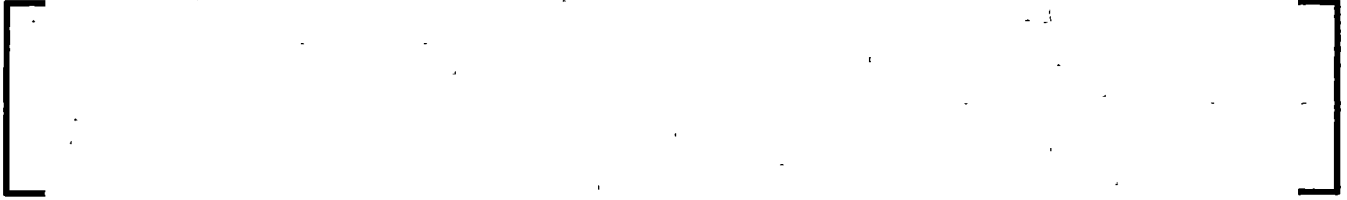
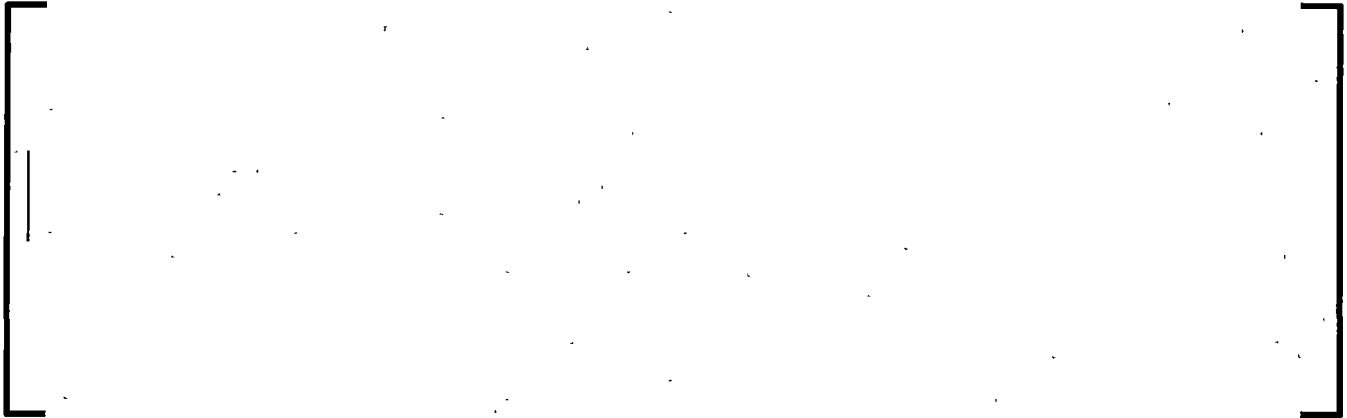**Table C-5: Grid External Stiffness, External Damping, and Strength**

[

]

Framatome Inc.

Deformable Spacer Grid Element
Topical Report

ANP-10337
Revision 0
Supplement 1NP
Revision 0
Page C-12

**Table C-6: Deformable Grid Element Input Parameters at Operating
Conditions**

Framatome Inc

Deformable Spacer Grid Element
Topical Report

ANP-10337
Revision 0
Supplement 1NP
Revision 0
Page C-13

Table C-7: Equivalent and Internal Spring Stiffness and Damping at Operating Conditions

Framatome Inc.

Deformable Spacer Grid Element
Topical Report

ANP-10337
Revision 0
Supplement 1NP
Revision 0
Page C-14

Table C-8: Mixed Core Deformable Grid Element Input Parameters at Operating Conditions

Framatome Inc.

Deformable Spacer Grid Element
Topical Report

ANP-10337
Revision 0
Supplement 1NP
Revision 0
Page C-15
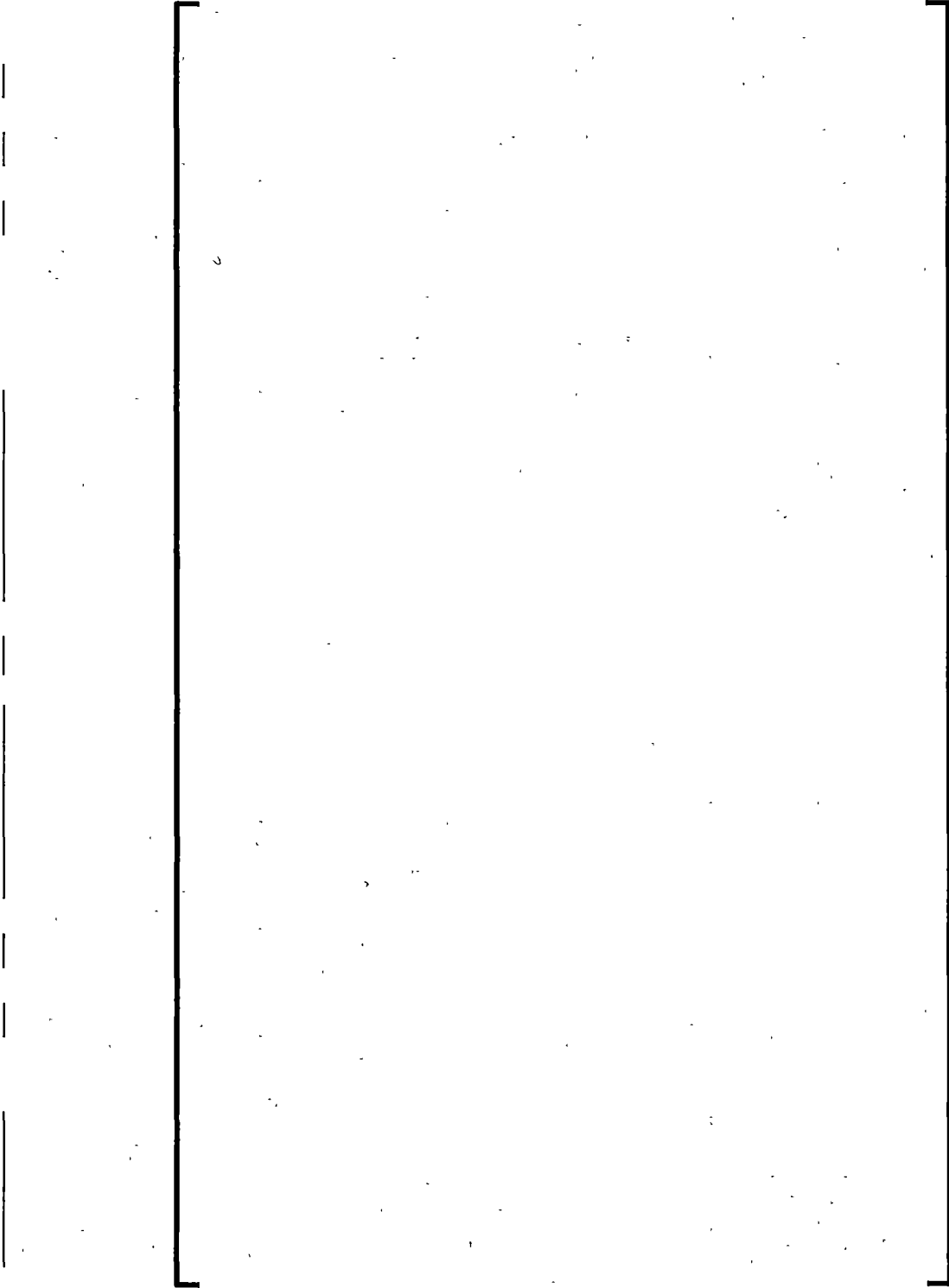
Table C-9: Spacer Grid Deformations, Full Core

Table C-10: IGM Impact Forces, Full Core

Framatome Inc.

Deformable Spacer Grid Element
Topical Report

ANP-10337
Revision 0
Supplement 1NP
Revision 0
Page C-16

Table C-11: Spacer Grid Deformations, Mixed Core

Table C-12: IGM Impact Forces, Mixed Core